Reply to RC1 on acp-2020-461

Taraborrelli *et al.*

December 23, 2020

Dear Anonymous Referee #1,

thank you for your thoughtful review of our manuscript. It helped us improving the manuscript considerably. Please find below a point-by-point response to your comments.

> ***Description***
> *This manuscript describes the changes in trace gas concentrations that occur when emissions of monocyclic aromatic compounds are included in a global general circulation / atmospheric chemistry model. Many recent studies have pointed out the strong influence of aromatic compounds on local and regional air quality, especially in East Asia, which makes this manuscript a timely assessment of their treatment in models and their global impacts. Here, the authors incorporate the MECCA mechanism into EMAC and diagnose the implications of aromatic chemistry by comparing a simulation with aromatic emissions turned on to one with aromatic emissions turned off. Unsurprisingly, they find that aromatic compounds contribute substantially to the global budgets of glyoxal and methylglyoxal – two of their main oxidation products and important SOA precursors – while their contributions to the budgets of smaller and more ubiquitous carbon-containing compounds, such as HCHO and CO, are smaller relative to the background. For budgets of HOx, NOx, and ozone, the effects are more complex; while aromatic emissions have small global effects (which, intriguingly, sometimes contradict those found by previous studies), their local effects can be moderately substantial and can vary in sign depending on local chemistry.*

Reply:
We appreciate Referee #1 for the accurate and synthetic summary of our manuscript.

> ***General comments***
> *The manuscript is straightforwardly written, well laid-out, and presents its findings clearly. Furthermore, because the authors use a highly comprehensive mechanism based on MCM, the chemical outcomes of aromatic oxidation are likely more robust than previous studies. However, it appears from looking more closely at the mechanism that some of the larger aromatic species (e.g. xylene and ethylbenzene) are not actually treated explicitly, but are oxidized in pathways identical to those of toluene with a "LCARBON" counter species denoting the carbon imbalance that arises from this treatment. This should be more explicitly described in the manuscript, which appears to imply that all aromatic species are treated independently by providing their individual emissions.*

Reply:
Indeed we have not made this aspect clear. In the model description (Section 2) we now stress this approximation and the error it may result from for prediction of stable products and low volatile compounds contributing to SOA formation.
We have added the text below at L75:

In short, the MCM schemes for benzene and toluene were taken. Following the approach of Taraborrelli et al. (2009), short-lived intermediates were replaced with their stable products and isomeric peroxy radicals were lumped preserving the yield of stable products. Initial oxidation steps of aromatics other than benzene and toluene are considered and products replaced by the analogous toluene oxidation products. This approximation inherently introduces an error with respect to the formation of larger and low volatile products. The carbon mass that is not accounted for with this approximation is however tracked by introducing the counter LCARBON for the difference of carbon atoms between the oxidation products of larger aromatics and toluene.

> *Another general concern is that in many places model outcomes are simply described without sufficient discussion of their causal pathways, which strongly diminishes the usefulness of these findings. Further, many of the important effects of these model outcomes are only touched on without any quantitative discussion – e.g., the changes to methane lifetime and SOA formation from glyoxal and methylglyoxal.*

Reply:
We have put significant efforts in discussing the results but we are happy to improve the manuscript in this respect by following specific indications. Concerning the first specific effect that Referee #1 pointed to, we acknowledge that the quantification of the impact on methane lifetime could have been given more space than a short mention without referring to Table 4. Therefore, we have extended the paragraph L129-132 by pointing explicitly to Table 4 and shortly discussing the changes in OH and CH4 lifetime in the two hemispheres.

The paragraph

Figure 5 shows the annual zonal mean changes of the OH mixing ratio. The changes are most pronounced in the NH upper troposphere where reductions range from 7 % to 20 %. This helps bringing the model-simulated inter-hemispheric OH asymmetry closer to that derived from observations (Lelieveld et al., 2016). Globally, aromatics oxidation reduces OH by 7.7 % and consequently increases methane lifetime.

has been extended:

Figure 5 shows the annual zonal mean changes of the OH mixing ratio. The changes are most pronounced in the NH upper troposphere where reductions range from 7 % to 20 %. These predicted changes are associated to similar reductions in NO_x. In fact, the upper troposphere is in general NO_x-limited and the oxidation of aromatics enhances the formation N_2O_5 and HNO_3 which are lost heterogeneously. This leads to an effective removal of NO_x from the gas phase and lowers the radical production. The change in hemispheric burdens of OH are consistent with this picture (Table 4). This moderately helps bringing the model-simulated inter-hemispheric OH asymmetry closer to that derived from observations (Lelieveld et al., 2016). Globally, aromatics oxidation reduces OH by 7.7 % and consequently increases methane lifetime by about 5.5 %. The changes are more pronounced in the northern hemisphere where aromatics are mostly emitted (Table 4). However, the latter in the EMAC model remains significantly lower than the ACCMIP multi-model mean and the observational-based estimates (Naik et al., 2013). Coarse model spatial resolutions (about 200 km) are known to result in an overestimation (underestimation) of global mean OH (methane lifetime) of at least 5 % (Yan et al., 2016). This is due to a less efficient conversion of NO_x to NO_y when strong pollutant emissions are artificially diluted in the model grid boxes. This aspect certainly has a larger impact on the inter-hemispheric OH asymmetry in atmospheric models that is in contrast to observational estimates (Patra et al., 2014).

With respect to the second specific effect Referee #1 pointed to, SOA formation from α-dicarbonyls, we think this is beyond the scope of the present manuscript for the following reason. The simulations were performed with a VBS-based approach to model condensation of organic vapours, at the time of writing of the manuscript no representation of oligomer formation from (methyl)glyoxal was implemented in the EMAC model yet. This is now implemented explicitly for cloud droplets (Rosanka et al., 2020) and its effect is planned to be assessed in a subsequent study together with the contribution of reactive uptake of epoxides from isoprene and aromatics. We have extended paragraph L201-209 by adding this explanation.

Specifically, we have extended

These changes are of significance for the model SOA budget since these two dicarbonyls are estimated to produce a large fraction of SOA by cloud processing (Lin et al., 2012).

These changes are of significance for the model SOA budget since these two dicarbonyls are estimated to produce a large fraction of SOA by cloud processing yielding low-volatile oligomers (Lin et al., 2012). However, a model assessment of SOA formation from α-dicarbonyls is beyond the scope of this study. The reason is that, although the simulations were performed with a VBS-based approach to model condensation of organic vapours, the EMAC model version used in this study has no representation of oligomer formation from (methyl)glyoxal. This has been recently implemented explicitly for cloud droplets (Rosanka et al., 2020) and its effect is planned to be assessed in a subsequent study together with the contribution of reactive uptake of epoxides from isoprene and aromatics.

> *Specific instances are pointed out in the comments below. Finally, while the short discussion of uncertainties in Section 4 is a particularly useful addition to this manuscript, it does not go far enough to provide the reader with either quantitative or qualitative bounds on the model outcomes described herein. Of particular note, more attention should be paid to:*
> *(a) the effects of grid resolution – given that there's a lot of spatial heterogeneity in model outcomes, and the effects even change sign depending on local conditions, is 1.875 square enough to resolve this chemistry? What outcomes might be masked by the artificial mixing that occurs in such large-scale grid boxes?*

Reply:
We thank the reviewer for pointing to this important aspect that, indeed, we have not mentioned in our manuscript. We gladly take this chance to discuss the influence of (horizontal) spatial resolution on the predicted changes of trace gas levels. We now shortly mention it in our extension of paragraph L129-132 concerning OH and methane lifetime . Moreover, we add a whole paragraph in Section 4 on model uncertainties in which we frame and formulate our expectation for modelled HO_x, NO_x and O_3.

The spatial resolution of atmospheric models has a significant influence on the predicted levels of oxidants and nitrogen oxides. Generally in polluted regions the coarser the resolution the larger the ozone production per molecule of NO_x will be (Sillman et al., 1990). This is due to the artificial dilution of strong NOx emissions which, in reality, is efficiently converted to NO_y by reacting with HO_x. For instance, reducing the spatial resolution over the polluted North America, Europe and East Asia with a two-way nested regional model led to a 9.5 % reduction in the global tropospheric ozone burden (Yan et al., 2016). We have shown that at our model resolution of 1.875° × 1.875° aromatics are estimated to induce important increases in HO_x (Fig. 3) and decreases in NO_x (Fig. 10 and 11) over continental polluted regions. Therefore, at much higher spatial resolutions we expect that the enhancement of surface ozone by aromatics in those regions (Fig. 6) to be greatly reduced if not reverted. Based on the results by Yan et al. (2016) we expect this effect to translate in a significant enhancement of the tropospheric ozone reduction reported in this study (Sect. 3.2). A quantification of the model resolution effect on chemical regimes is at the moment computationally prohibitive with our very large chemical scheme running in the global EMAC model.

> *(b) uncertainties in chemical mechanisms, especially the newly implemented ones de-*

> *scribed in the bullet point list in Section 2 –while there is some discussion in Section 4 of the uncertainty in the phenoxy + O3 reaction, it should be put into a larger context and more explicitly tied to the uncertainty bounds of model outcomes that might be expected given the uncertainties in the chemical mechanism;*

Reply:
We agree with Referee #1. We have expanded Section 4 by discussing the uncertainties associated with the limitations of currently accepted oxidation mechanisms like the MCM. Specifically, we now mention the uncertainty on the epoxide formation pathway that is treated as direct in the MCM. This likely involves intermediate steps implying an epoxide yield dependent on NO_x and HO_x levels (Vereecken, 2019).

We have added the paragraph below:

Another source of uncertainty is the direct formation of epoxide upon addition of OH and subsequently by O_2 as implemented in the MCM ranging from 11.8 %, for benzene, to 24 %, for trimethylbenzene (Bloss et al., 2005b,a). There in fact consistent theoretical evidence that the epoxide formation pathway passes through a second O_2-addition. This implies that the epoxide yield likely depends on the abundance of $NO, HO_2 and RO_2$ (Vereecken, 2019, and references therein). This uncertainty limit the reliability of the predicted SOA formation from reactive uptake of epoxides by aerosols (Paulot et al., 2009).

> *and lastly (c) uncertainties in emissions – while these are also discussed briefly in Section 4, the scope of the discussion is very limited and does not leave readers with any quantitative understanding of how well the emission totals are known, what their overall inter-annual variability might be, and how this could affect the model outcomes described in Section 3. I am not trying to argue that the authors need to perform additional sensitivity simulations, but the uncertainties merit a more lengthy,detailed, and quantitative description than is provided here.*

Reply:
We agree with Referee #1 and therefore we expanded paragraph L243-247 of Section 4 by discussing magnitude and inter-annual variability of aromatics emissions from biomass burning, anthropogenic activities and terrestrial vegetation.

We have added the paragraph below:

However, it appears that the two major contributions to this variability are the peat fires in Indonesia and boreal forest fires, which are strongly favoured by El Nino and heat waves, respectively. An early estimate of anthropogenic emissions of aromatics gave 16 TgC/a, (Fu et al., 2008). Two relatively recent datasets yield about 50% higher emissions being 23 TgC/a for RCP (Cabrera-Perez et al., 2016) and 22 TgC/a for EDGAR 4.3.2 (Huang et al., 2017). The latter is used in this study and lacks the biofuel burning emissions of phenol, benzaldehyde and styrene. Inter-annual variability of anthropogenic emissions of aromatics is is not well known but the decadal trends are known to be negative since the 1980s (Lamarque et al., 2010). Aromatics emissions from terrestrial vegetation have been long neglected or considered very low. However, Misztal et al. (2015) suggested that aromatics emissions from biogenic sources may rival those from anthropogenic ones. In this study we used the same emission algorithm used in Misztal et al. (2015) but get much lower emissions for toluene (about 0.3 vs. 1.5 TgC/a). However, Misztal et al. (2015) suggest that emissions of aromatics and benzenoid compounds may be in the 1.4-15 TgC/a range. The major contributors are toluene and some benzenoids (oxygenated aromatics). The latter are mainly emitted during blossoming and stress-induced reactions by plants. The variability of their emissions is not very well quantified. For instance, the MEGAN model calculates their emission strengths based of the ones for carbon monoxide (Tarr et al., 1995).

> ***Specific Comments***
> *Additional (more specific)questions about uncertainty are given below.*
> *L 19 - Does the 200-300 Tg/yr refer to Tg O3?*

Reply:
Yes, it does. We believe that in the relative sentence it is clear that we refer to O_3.

> *L 69-72 - Because the primary findings of this paper rely so heavily on the magnitude of these emissions, some small discussion of their uncertainty is warranted. Do the sources from which the inventories were derived describe the range of plausible emission amounts? Do different anthropogenic or biomass burning inventories give different emission amounts? EDIT - I see this is partially addressed in Section 4 (though it would be useful here to direct the reader to the later discussion of uncertainties). However,the short paragraph about emissions uncertainties still lacks quantitative detail, and most of the questions above still remain unanswered. Also, can a numerical range of inter-annual variability of total pyrogenic aromatic emissions be provided?*

Reply:
Referee #2 made a similar point in the general comment above. We agree and have expanded the relative paragraph in Section 4 and mentioned in our reply above.

> *L 75 - It would be helpful here to give detail not only on the additions that have been to the mechanism, but also on generally what simplifications were made to MCM to arrive at MECCA. I realize that's available in Cabrera-Perez et al. 2016, but the reader should be able to get a sense of the methodology here without having to fully read another paper. In particular, it is problematic that this manuscript implies a full detailed mechanism for the suite of aromatics shown in Table 1 when in fact many of them just use the same oxidation schemes.*

Reply:
We thank Referee #1 for making us aware of this aspect. For that we have added a short description of the simplifications made to the MCM mechanism for benzene and toluene. This is now combined with the mentioning of the LCARBON species counter as requested in your general comment.

> *L 122-124 - This is not a complete explanation of the OH increase in high-NOx regions. It is stated that the increased OH is "caused by the reaction of NO with HO2", but it was also stated two lines previously that NO decreases in these regions. Does HO2 increase enough as to offset both the NO decrease and the OH decrease through direct reaction with aromatics? What causes such a pronounced HO2 increase? Further,Figures 4 and 5 are not particularly useful to the reader without an explanation of why these effects occur. What causes the seasonal variability in the effects of aromatics on OH? Why are they strongest in the upper troposphere?*

Reply:
The increase in HO_2 indeed overcompensates for the decrease in NO resulting in enhanced OH levels over regions where radical production is not NO_x-limited. The HO_2 production from VOC oxidation is a well established knowledge in atmospheric chemistry. In *AROM* compared to *onlyMCM* this production is further enhanced by the photolysis of ortho-nitrophenols and benzaldehyde that we have mentioned in the manuscript. We have modified the manuscript in order to make this point clear.

The paragraph

We find a positive correlation between OH and anthropogenic emissions in these regions but a negative correlation in the low-NO_x CAF region. The increased OH in the high-NO_x regions is mainly caused by the reaction of NO with HO_2.

has been modified to

We find that inclusion of aromatics emissions leads to an increase OH in these regions but to decrease in the low-NO_x CAF region. The increased OH in the high-NO_x regions is mainly caused by the reaction of NO with HO_2. The production of OH from this important reaction is enhanced by the significant HO_2 formation in aromatics oxidation. Compared to *onlyMCM* the *AROM* simulation has additional HO_2 production from the photolysis of ortho-nitrophenols (R1) and benzaldehyde (Sect. 2). The enhanced HO_2 levels (not shown) overcompensates the negative changes in NO (see Sect. 3.2).

With respect to Figure 4 we have added a brief explanation of why the largest decrease in planetary boundary OH is computed for the NH.

In general enhancements are predicted for regions where radical production is not NO_x-limited. In the NH there obviously more such regions compared to the SH. However, the largest decrease in the planetary boundary OH is computed for the NH where most of the emissions of aromatics are located.

With respect to Figure 5 we have added an explanation for the reduced OH levels in the upper troposphere. The predicted changes are associated to similar reductions in NO_x. In fact, the upper troposphere is in general NO_x-limited and the oxidation of aromatics enhances the formation N_2O_5 and HNO_3 which are lost heterogeneously. This leads to an effective removal of NO_x from the gas phase and lowers the radical production.

We have extended the text below

Globally, aromatics oxidation reduces OH by 7.7 % and consequently increases methane lifetime.

with

Globally, aromatics oxidation reduces OH by 7.7 % and consequently increases methane lifetime by about 5.5 %. The changes are more pronounced in the northern hemisphere where aromatics are mostly emitted (Table **??**). However, the latter in the EMAC model remains significantly lower than the ACCMIP multi-model mean and the observational-based estimates (Naik et al., 2013). Coarse model spatial resolutions (about 200 km) are known to result in an overestimation (underestimation) of global mean OH (methane lifetime) of at least 5 % (Yan et al., 2016). This is due to a less efficient conversion of NO_x to NO_y when strong pollutant emissions are artificially diluted in the model grid boxes. This aspect certainly has a larger impact on the inter-hemispheric OH asymmetry in atmospheric models that is in contrast to observational estimates (Patra et al., 2014).

> *L 123 - Is this "positive correlation" a quantitative effect, diagnosed by some sort of regression analysis (across time? or just regions?), and if so, can it be explained in more detail here? If this "positive correlation" is just meant to say that including anthropogenic emissions causes an increase in OH, then this phrasing is misleading – better just to state simply that OH is higher in AROM than NOAROM in these regions. Also,are these correlations really diagnosed from anthropogenic emissions in particular, or from the inclusion of all aromatic emissions (including biogenic and pyrogenic)?*

Reply:
We apologize for this misleading formulation. We have modified the sentence as suggested by the Referee by removing the use of the word "correlation".

> *L 132 - The increased methane lifetime is likely to be of great interest to readers. Can it be quantified?*

Reply:
It is quantified and also broken down for the two hemispheres in Table 4. As mentioned in the reply to the general comments above, we expanded paragraph L129-132 in which we have made an explicit reference to Table 4 and quantify the change in calculated methane lifetime.

> *L 138-140 - The same comment above (L 123) applies here to the "correlation" phrasing.*

Reply:
We apologize again for the misleading formulation and have changed the text similarly as mentioned in the answer above.

> *L 141 - It appears Figure 9 is discussed here in the text before Figures 7 (L 143) and 8 (L157)*

Reply:
Thank you for pointing to this. We fixed it in the revised manuscript.

> *L 141-145 - The same comment above (L 122-124) applies here; why do these seasonal and zonal patterns arise?*

Reply:
The inter-hemispheric changes in O_3 are indeed similar, although much less pronounced, and not independent from the changes in OH. In the revised manuscript we describe it and stress more the connection to changes in OH.

We have added the sentence

Like for the OH levels, the inter-hemispheric asymmetry in the emission of aromatics determines the higherO_3 decrease in the NH compared to the SH.

> *L 153 - Can some more quantitative description of the variation with tropopause definition (and a description of the definition itself) be included here? What specifically is meant by "robust"? Figure 7 makes it look instead like there are large absolute differences right at the tropopause, which would imply that the definition might be highly important.*

Reply:
We have extended the caption of Table 4 by listing all 6 different definitions and diagnostic "tropopauses" that are calculated by EMAC with the MESSy submodel TROPOP (Jöckel et al., 2010). In the caption we also report that the results do not change by more than 0.05 %.

The caption of Table 4 has been extended with the text below

Tropospheric burdens were reckoned using six different tropopause definitions (provided by the TROPOP submodel, see Jöckel et al. (2010) for details): 1,2 surfaces of O_3 mixing ratio of 125 and 150 nmol/mol, respectively, 3) WMO definition (WMO (1957)), 4) dynamic PV-based (3.5 PVU potential vorticity surface, sought within 50–800 hPa), 5) climatological (invariable zonal profile, i.e. $300\text{-}215\bullet(\cos(\text{latitude}))^2$ hPa) and 6) the combined definition (WMO tropopause within 30°N–30°S, otherwise dynamic PV-based tropopause). The latter definition is used by default in EMAC and in this work. Estimated changes to tropospheric O_3 burden are identical within 0.05 % between the available definitions.

> *L 154 - What is meant by "these changes", and why does the explanation provided here differ from those above (L 134-136)?*

Reply:
We acknowledge the inconsistency and the lack of clarity of this formulation. What we wanted to highlight is the direct ozone loss by reaction with (substituted) phenoxy radicals that we find to play as an **additional** and previously overlooked ozone sink at global scale. We have now reformulated the corresponding sentence in this sense.

We have changed the sentence

These changes are associated with the enhanced direct ozone loss by reactions with organic compounds.

to

The changes in ozone are caused by perturbations of the radical production in different NO_x regimes but also by the direct ozone loss in reactions with organic compounds.

> *L 159 - Extra close-parentheses.*

Reply:
Corrected.

> *L 143-164 - This paragraph is long and covers a wide range of different topics; consider splitting it up? Also, the sentences around L 156-160 seem to be in an odd order; the sentence beginning "However, with aromatics" seems like it should be followed by the sentence beginning "Ozone is known to react", while the two intervening sentences seem like a non sequitur.*

Reply:
We thank the Referee #1 for this comment. We now split the long paragraph where we start discussing the direct losses of ozone in the oxidation of organic compounds. Our sentence beginning with "However, with aromatics" is meant to stress that all the other global atmospheric chemistry models do not represent additional direct loss of ozone in VOC oxidation. We hope that our explanation clarifies the issue.

> *L 161-164 - How well is this chemistry known? The cited study describes the reactions of the phenoxy radical with O3 and with other phenoxy radicals, but presumably this is also in competition with many other reactions, including possible unimolecular re-arrangements or decomposition. Have competitive studies been reported? If not, can some estimate of competing reactions rates be used along with the uncertainty bounds of the phenoxy + ozone reaction rate to determine some level of certainty for this discussion here? Considering how strong the simulated effect is, and how its catalytic nature under some conditions could magnify even small errors, some discussion of uncertainty is warranted. EDIT - I see this is partially addressed below in section 4 (it'd be nice to have some parenthetical here directing the reader to the later discussion on uncertainties). Some questions remain, though – most notably why the rate constant"has to be regarded as a lower limit" (L 227) and whether competing reactions might also be uncertain.*

Reply:
We thank the Referee #1 for this useful comment. The chemistry of phenoxy radicals is indeed not

very well known. The rate constant for the reaction with ozone has been determined at only ambient temperature. The latter is a lower limit because of the nature of the kinetic experiments and analysis conducted by Tao and Li (1999). Phenoxy radical is very stable radical and the only other known sink is the reaction with NO_2, which yields ortho-nitrophenols. The rate constant of the latter reaction is about one order of magnitude higher. However, ozone is very often more abundant than NO_2 by more than an order of magnitude. This makes ozone to our knowledge the major atmospheric sink for phenoxy radicals. The reaction with NO is reversible and not considered neither in MCM nor in our mechanism. We have mentioned these additional sinks for phenoxy in the manuscript. However, we did not mention the relative magnitude of the rate constants and neither did we make a statement about ozone being the major atmospheric sink of phenoxy radicals. We now mention this aspect in the revised manuscript and have added a reference to the discussion of the mechanistic uncertainties in Section 4.

We have modified the sentence in L166-167

This ozone loss is enhanced by phenoxy radical production in the R2 reaction and the subsequent loss of odd oxygen by NO_3 photolysis and N_2O_5 heterogeneous loss

to

Although the known rate constant for reaction R3 is about one order of magnitude lower than the others, the high abundance in the atmosphere makes ozone the major sink of (substituted) phenoxy radicals. This direct ozone loss in reaction R3 is enhanced by phenoxy radical production in reaction R2 and the concurrent loss of odd oxygen by NO_3 photolysis and N_2O_5 heterogeneous loss

> *L 164 - No period (assuming this is the end of the sentence).*

Reply:
Yes, we now close the sentence with a column.

> *L 173-174 - How does nitrophenol photolysis come into play here for the phenoxy radicals? R1 implies either that nitrophenol photolysis does not form phenoxy radicals or that the mechanism skips the phenoxy radical step and goes directly to decomposition products.*

Reply:
The HONO-channel in the photolysis of ortho-nitrophenols is predicted to form phenyloxy radicals which likely rearrange to a 7-membered ring radical and further decomposes (Vereecken et al., 2016). Formation of phenoxy radicals from photolysis of ortho-nitrophenols is not skipped. However, we acknowledge that the OH-channel, which may be much more important of the HONO-channel, produce nitrosophenoxy radicals might efficiently react with ozone similarly as phenoxy radicals. However, this chemistry is unknown. In Section 3.2 we now refer to Section 4 where we already discuss these mechanistic uncertainties.

> *L 186-187 - This phrasing does not make it particularly clear which simulation has the higher NO3 concentrations.*

Reply:
Indeed it is not clear. We have modified the first part of the sentence by starting with ”Relative to *NOAROM*, in *AROM* ...”

> *L 188 - Why does this effect occur in places with pyrogenic aromatic emissions, while the HOx and O3 effects described previously are more strongly associated with anthropogenic emissions? The same question applies to the HONO increase on L 191.*

Reply:
We are not sure why these decreases are predicted and suppose is a result of a complex interplay of multiple factors. Thus, we refrain to make statements not backed by a solid understanding. We added to the manuscript that these changes are modest and stress more the widespread increase of NO_3 levels by the reaction of phenyl peroxy radicals with NO_2.

We have modified the sentence at L189 from

Comparing *AROM* to *NOAROM*, the global average of the nighttime species NO_3 increases by more than 7 % (Tab. 3).

to

However the latter seems to dominate and cause a significant and widespread increase in the predicted NO_3 levels. Relative to *NOAROM*, in *AROM* the global average of the nighttime species NO_3 increases by more than 7 % (Table 3).

> *L 198-200 - What is the explanation for these findings?*

Reply:
We think this is due to the concurrent enhancement of OH levels which "curb" the enhancement of HCHO in China, Europe and US. We have modified the text in order to express this explanation.

We have expanded the relative sentence to

There are, however, regional differences that are moderate because of the concurrent enhancement of the HCHO sink by reaction with OH.

> *L 208-209 - Was the effect on the SOA budget quantified here? It seems this effect would be of great interest to some readers.*

Reply:
No, it was not quantified in this study. However, it will be subject of future studies in which the production of oligomers from dicarbonyls in the condensed phase is represented. Recently, we have added the cloud processing of dicarbonyls to the scavenging module of MESSy (Rosanka et al., 2020) and will evaluate the impact of it on the SOA budget in a future study.

> *L 218 - It seems odd that so much detail is shown in the many other figures for other species discussed in this manuscript, but this interesting finding for CO is not shown.Can a CO figure be added, and can an explanation be given for these spatial effects?*

Reply:
We understand Referee #1 but we had the feeling we had already too many figures in the manuscript. We are happy to add to the manuscript the figure showing the zonal mean differences for CO which peak in the NH UTLS.

> *L 230-231 - It was earlier implied (L 173-174) that the model *does* account for the effects of photolysis of nitrophenols. Can this be clarified?*

Reply:
The model accounts for the known photolysis of ortho-nitrophenols yielding HONO. However, our

model does not account for the less known OH-channel potentially yielding nitrosophenoxy radicals (Vereecken et al., 2016), which might react similarly as phenoxy radicals. At the time of finalizing the chemical mechanism we were not aware of the results by Vereecken et al. (2016). Nevertheless, we state clearly in Section 4 that our model lacks photolysis of nitrophenols yielding phenoxy radicals. In this section we have replaced "reforming phenoxy radicals" with "forming nitrosophenoxy radicals".

> ***Technical comments***
> *Table 5 is cut off by the end of the page.*

Reply:
We apologize for this inconvenient. The table is not cut off in the ACP article layout. We report the complete table here at the end of the document (see Table 1).

> *Can the OH mixing ratios in Figures 3-5 be expressed instead in the more commonly used concentration units?*

Reply:
We know that OH abundance in the atmosphere is usually expressed in molec cm^{-3}. However, doing it in our manuscript would introduce an exception and an inconsistency to the way we present the results. For this reason we would like not to modify the units.

> *Figure 4 is very confusing. What are the units on the left plot? Why are there two very close blue and red lines in the left plot? Why does the caption reference solid and dashed lines in the right plot when only solid lines exist? The same questions apply to Figure 9.*

Reply:
In all Figures of this manuscript, the plotted values correspond to the original output values in mol/mol multiplied by ten to a certain power. For example, the values on the vertical axis of Fig. 4 (left) stand for mol/mol multiplied by 1e+14. Since this notation is not intuitive, we changed the titles of the plots and added the unit (e.g. "x 10^{-11} mol/mol").
The caption is indeed not clear, as the dashed and solid lines are only in the left plot of Fig. 4 and Fig. 9 (they distinguish the results of AROM and NOAROM). We changed the caption of Fig. 4 to: "Left: Seasonal cycles of OH daily (24 h) mixing ratio means (in 10^{-14} mol/mol) in the planetary boundary layer (PBL) for AROM (solid line) and NOAROM (dashed line). Right: Relative difference (expressed in %) between AROM and NOAROM. In blue, values for the NH; in red, values for the SH...." We changed the caption of Fig. 9 to: "Same as in Fig. 4 for ozone (the unit in the left plot is 10^{-8} mol/mol).

References

Bloss, C., Wagner, V., Bonzanini, A., Jenkin, M. E., Wirtz, K., Martin-Reviejo, M., and Pilling, M. J.: Evaluation of detailed aromatic mechanisms (MCMv3 and MCMv3.1) against environmental chamber data, Atmos. Chem. Phys., 5, 623–639, https://doi.org/10.5194/acp-5-623-2005, URL `https://www.atmos-chem-phys.net/5/623/2005/`, 2005a.

Bloss, C., Wagner, V., Jenkin, M. E., Volkamer, R., Bloss, W. J., Lee, J. D., Heard, D. E., Wirtz, K., Martin-Reviejo, M., Rea, G., Wenger, J. C., and Pilling, M. J.: Development of a detailed chemical mechanism (MCMv3.1) for the atmospheric oxidation of aromatic hydrocarbons, Atmos. Chem. Phys., 5, 641–664, https://doi.org/10.5194/acp-5-641-2005, 2005b.

Cabrera-Perez, D., Taraborrelli, D., Sander, R., and Pozzer, A.: Global atmospheric budget of simple monocyclic aromatic compounds, Atmos. Chem. Phys., 16, 6931–6947, https://doi.org/10.5194/acp-16-6931-2016, 2016.

Table 1: Regionally averaged mixing ratios of selected species (annual averages for 2010).

	NOAROM	*AROM*	ABSDIFF	RELDIFF
	mol/mol	mol/mol	mol/mol	%
		OH		
AMA	2.861×10^{-14}	2.785×10^{-14}	-7.689×10^{-16}	-2.687
CAF	6.447×10^{-14}	6.086×10^{-14}	-3.616×10^{-15}	-5.608
EAS	4.712×10^{-14}	5.527×10^{-14}	8.147×10^{-15}	17.29
EUR	3.591×10^{-14}	3.852×10^{-14}	2.615×10^{-15}	7.283
EUS	5.629×10^{-14}	5.784×10^{-14}	1.553×10^{-15}	2.759
		O_3		
AMA	2.979×10^{-8}	2.909×10^{-8}	-6.973×10^{-10}	-2.341
CAF	3.856×10^{-8}	3.712×10^{-8}	-1.440×10^{-9}	-3.733
EAS	3.124×10^{-8}	3.505×10^{-8}	3.807×10^{-9}	12.19
EUR	3.045×10^{-8}	3.033×10^{-8}	-1.250×10^{-10}	-0.4105
EUS	3.930×10^{-8}	3.904×10^{-8}	-2.604×10^{-10}	-0.6626
		NO_3		
AMA	3.570×10^{-13}	3.483×10^{-13}	-8.678×10^{-15}	-2.431
CAF	2.105×10^{-12}	2.321×10^{-12}	2.163×10^{-13}	10.27
EAS	1.833×10^{-12}	1.949×10^{-12}	1.163×10^{-13}	6.346
EUR	1.280×10^{-12}	1.256×10^{-12}	-2.448×10^{-14}	-1.913
EUS	2.536×10^{-12}	2.488×10^{-12}	-4.802×10^{-14}	-1.894
		HONO		
AMA	5.335×10^{-11}	5.349×10^{-11}	1.370×10^{-13}	0.2567
CAF	8.110×10^{-11}	8.227×10^{-11}	1.174×10^{-12}	1.447
EAS	1.152×10^{-10}	1.038×10^{-10}	-1.146×10^{-11}	-9.945
EUR	5.689×10^{-11}	5.604×10^{-11}	-8.429×10^{-13}	-1.482
EUS	4.415×10^{-11}	4.230×10^{-11}	-1.854×10^{-12}	-4.199
		HNO_3		
AMA	1.515×10^{-10}	1.508×10^{-10}	-7.056×10^{-13}	-0.4657
CAF	4.957×10^{-10}	5.162×10^{-10}	2.048×10^{-11}	4.131
EAS	1.035×10^{-9}	1.169×10^{-9}	1.335×10^{-10}	12.89
EUR	3.985×10^{-10}	4.003×10^{-10}	1.855×10^{-12}	0.4656
EUS	6.706×10^{-10}	6.721×10^{-10}	1.505×10^{-12}	0.2244
		HCHO		
AMA	5.217×10^{-9}	5.189×10^{-9}	-2.874×10^{-11}	-0.5509
CAF	3.468×10^{-9}	3.478×10^{-9}	9.392×10^{-12}	0.2708
EAS	1.322×10^{-9}	1.557×10^{-9}	2.348×10^{-10}	17.76
EUR	7.356×10^{-10}	7.708×10^{-10}	3.517×10^{-11}	4.781
EUS	1.911×10^{-9}	1.942×10^{-9}	3.096×10^{-11}	1.620
		glyoxal		
AMA	1.473×10^{-10}	1.514×10^{-10}	4.120×10^{-12}	2.797
CAF	7.507×10^{-11}	1.169×10^{-10}	4.180×10^{-11}	55.68
EAS	3.077×10^{-11}	1.119×10^{-10}	8.112×10^{-11}	263.6
EUR	1.410×10^{-11}	3.271×10^{-11}	1.861×10^{-11}	132.0
EUS	6.217×10^{-11}	8.121×10^{-11}	1.904×10^{-11}	30.63
		methyl glyoxal		
AMA	8.078×10^{-10}	8.021×10^{-10}	-5.711×10^{-12}	-0.7070
CAF	2.684×10^{-10}	2.802×10^{-10}	1.176×10^{-11}	4.383
EAS	5.081×10^{-11}	9.389×10^{-11}	4.308×10^{-11}	84.80
EUR	2.214×10^{-11}	3.157×10^{-11}	9.425×10^{-12}	42.57
EUS	1.938×10^{-10}	2.036×10^{-10}	9.750×10^{-12}	5.031

Fu, T.-M., Jacob, D. J., Wittrock, F., Burrows, J. P., Vrekoussis, M., and Henze, D. K.: Global budgets of atmospheric glyoxal and methylglyoxal, and implications for formation of secondary organic aerosols, J. Geophys. Res., 113D, 2008.

Huang, G., Brook, R., Crippa, M., Janssens-Maenhout, G., Schieberle, C., Dore, C., Guizzardi, D., Muntean, M., Schaaf, E., and Friedrich, R.: Speciation of anthropogenic emissions of non-methane volatile organic compounds: a global gridded data set for 1970–2012, Atmos. Chem. Phys., 17, 7683–7701, https://doi.org/10.5194/acp-17-7683-2017, 2017.

Jöckel, P., Kerkweg, A., Pozzer, A., Sander, R., Tost, H., Riede, H., Baumgaertner, A., Gromov, S., and Kern, B.: Development cycle 2 of the Modular Earth Submodel System (MESSy2), Geosci. Model Dev., 3, 717–752, https://doi.org/10.5194/GMD-3-717-2010, 2010.

Lamarque, J.-F., Bond, T. C., Eyring, V., Granier, C., Heil, A., Klimont, Z., Lee, D., Liousse, C., Mieville, A., Owen, B., Schultz, M. G., Shindell, D., Smith, S. J., Stehfest, E., Van Aardenne, J., Cooper, O. R., Kainuma, M., Mahowald, N., McConnell, J. R., Naik, V., Riahi, K., and van Vuuren, D. P.: Historical (1850–2000) gridded anthropogenic and biomass burning emissions of reactive gases and aerosols: methodology and application, Atmospheric Chemistry and Physics, 10, 7017–7039, https://doi.org/10.5194/acp-10-7017-2010, URL `https://acp.copernicus.org/articles/10/7017/2010/`, 2010.

Lelieveld, J., Gromov, S., Pozzer, A., and Taraborrelli, D.: Global tropospheric hydroxyl distribution, budget and reactivity, Atmos. Chem. Phys., 16, 12 477–12 493, https://doi.org/10.5194/acp-16-12477-2016, 2016.

Lin, G., Penner, J. E., Sillman, S., Taraborrelli, D., and Lelieveld, J.: Global modeling of SOA formation from dicarbonyls, epoxides, organic nitrates and peroxides, Atmos. Chem. Phys., 12, 4743–4774, https://doi.org/10.5194/acp-12-4743-2012, 2012.

Misztal, P., Hewitt, C., Wildt, J., Blande, J., Eller, A., Fares, S., Gentner, D., Gilman, J., Graus, M., Greenberg, J., Guenther, A., Hansel, A., Harley, P., Huang, M., Jardine, K., Karl, T., Kaser, L., Keutsch, F., Kiendler-Scharr, A., Kleist, E., Lerner, B., Li, T., Mak, J., Nölscher, A., Schnitzhofer, R., Sinha, V., Thornton, B., Warneke, C., Wegener, F., Werner, C., Williams, J., Worton, D., Yassaa, N., and Goldstein, A.: Atmospheric benzenoid emissions from plants rival those from fossil fuels, Scientific Reports, 5, https://doi.org/10.1038/srep12064, 2015.

Naik, V., Voulgarakis, A., Fiore, A. M., Horowitz, L. W., Lamarque, J.-F., Lin, M., Prather, M. J., Young, P. J., Bergmann, D., Cameron-Smith, P. J., Cionni, I., Collins, W. J., Dalsøren, S. B., Doherty, R., Eyring, V., Faluvegi, G., Folberth, G. A., Josse, B., Lee, Y. H., MacKenzie, I. A., Nagashima, T., van Noije, T. P. C., Plummer, D. A., Righi, M., Rumbold, S. T., Skeie, R., Shindell, D. T., Stevenson, D. S., Strode, S., Sudo, K., Szopa, S., and Zeng, G.: Preindustrial to present-day changes in tropospheric hydroxyl radical and methane lifetime from the Atmospheric Chemistry and Climate Model Intercomparison Project (ACCMIP), Atmospheric Chemistry and Physics, 13, 5277–5298, https://doi.org/10.5194/acp-13-5277-2013, URL `https://acp.copernicus.org/articles/13/5277/2013/`, 2013.

Patra, P. K., Krol, M. C., Montzka, S. A., Arnold, T., Atlas, E. L., Lintner, B. R., Stephens, B. B., Xiang, B., Elkins, J. W., Fraser, P. J., Ghosh, A., Hintsa, E. J., Hurst, D. F., Ishijima, K., Krummel, P. B., Miller, B. R., Miyazaki, K., Moore, F. L., Mühle, J., O'Doherty, S., Prinn, R. G., Steele, L. P., Takigawa, M., Wang, H. J., Weiss, R. F., Wofsy, S. C., and Young, D.: Observational evidence for interhemispheric hydroxyl-radical parity, Nature, 513, 219–223, https://doi.org/10.1038/nature13721, URL `https://doi.org/10.1038/nature13721`, 2014.

Paulot, F., Crounse, J. D., Kjaergaard, H. G., Kürten, A., St. Clair, J. M., Seinfeld, J. H., and Wennberg, P. O.: Unexpected epoxide formation in the gas-phase photooxidation of isoprene, Science, 325, 730–733, https://doi.org/10.1126/science.1172910, 2009.

Rosanka, S., Sander, R., Wahner, A., and Taraborrelli, D.: Oxidation of low-molecular weight organic compounds in cloud droplets: development of the JAMOC chemical mechanism in

CAABA/MECCA (version 4.5.0gmdd), Geoscientific Model Development Discussions, 2020, 1–18, https://doi.org/10.5194/gmd-2020-337, URL `https://gmd.copernicus.org/preprints/gmd-2020-337/`, 2020.

Sillman, S., Logan, J. A., and Wofsy, S. C.: The sensitivity of ozone to nitrogen oxides and hydrocarbons in regional ozone episodes, J. Geophys. Res., 95D, 1837–1851, https://doi.org/10.1029/JD095iD02p01837, 1990.

Tao, Z. and Li, Z.: A kinetics study on reactions of C_6H_5O with C_6H_5O and O_3 at 298 K, Int. J. Chem. Kinet., 31, 65–72, https://doi.org/10.1002/(SICI)1097-4601(1999)31:1⟨65::AID-KIN8⟩3.0.CO;2-J, 1999.

Taraborrelli, D., Lawrence, M. G., Butler, T. M., Sander, R., and Lelieveld, J.: Mainz Isoprene Mechanism 2 (MIM2): an isoprene oxidation mechanism for regional and global atmospheric modelling, Atmos. Chem. Phys., 9, 2751–2777, https://doi.org/10.5194/ACP-9-2751-2009, 2009.

Tarr, M. A., Miller, W. L., and Zepp, R. G.: Direct carbon monoxide photoproduction from plant matter, Journal of Geophysical Research: Atmospheres, 100, 11 403–11 413, https://doi.org/https://doi.org/10.1029/94JD03324, URL `https://agupubs.onlinelibrary.wiley.com/doi/abs/10.1029/94JD03324`, 1995.

Vereecken, L.: Reaction Mechanisms for the Atmospheric Oxidation of Monocyclic Aromatic Compounds, chap. Chapter 6, pp. 377–527, World Scientific Publishing, https://doi.org/10.1142/9789813271838_0006, URL `https://www.worldscientific.com/doi/abs/10.1142/9789813271838_0006`, 2019.

Vereecken, L., Chakravarty, H. K., Bohn, B., and Lelieveld, J.: Theoretical study on the formation of H- and O-atoms, HONO, OH, NO, and NO_2 from the lowest lying singlet and triplet states in ortho-nitrophenol photolysis, Int. J. Chem. Kinet., 48, 785–795, https://doi.org/10.1002/kin.21033, 2016.

WMO: Definition of the tropopause and of significant levels, URL `https://library.wmo.int/doc_num.php?explnum_id=6960`, 1957.

Yan, Y., Lin, J., Chen, J., and Hu, L.: Improved simulation of tropospheric ozone by a global-multi-regional two-way coupling model system, Atmospheric Chemistry and Physics, 16, 2381–2400, https://doi.org/10.5194/acp-16-2381-2016, URL `https://acp.copernicus.org/articles/16/2381/2016/`, 2016.

Reply to RC2 on acp-2020-461

Taraborrelli *et al.*

December 23, 2020

Dear Alexander Archibald (Referee #2),

thank you for taking the time to review of our manuscript. It gave us the chance to improve the manuscript significantly.
Please find below a point-by-point response to your comments.

> ***Description***
> *Taraborrelli et al. provide an updated mechanism for the oxidation of aromatics in the EMAC model and a summary of the impacts of this update on key trace gases in the troposphere.This is a generally well written and well executed study but I have several minor comments in the attached pdf and a few more major comments before recommending publication.*

> ***Major comments***
> *Comparison to observations is lacking which limits the sense I get that the changes are in anyway in the right direction. For example, the changes in surface ozone and NO2 in EAS are large and I would imagine significant. It would be good to see how these compare with observations. Whilst I agree with the previous reviewers comments about model resolution and whilst there may well be structural errors in EMAC that mean that even with a better representation of the chemistry the comparison to observations is worse, I feel some comparison to observations is warranted.*

Reply:
We agree with the referee that comparison with observations would strengthen and focus the manuscript. However, a comprehensive evaluation of the EMAC model with the complex organic chemistry (MOM) and against satellite retrievals of O_3 and NO_2 is in preparation and will be soon submitted for peer review. A first comparison of the model results with IASI-FORLI retrievals for ozone along with a detailed O_x budget is currently presented in Rosanka et al. (2020). The model results for tropospheric ozone, with the modified MCM chemistry of aromatics we present here, are clearly still too high with overestimates of up to 10 DU. This positive bias will be addressed by further improving existent parametrizations in EMAC like the dry deposition scheme (Emmerichs et al., 2020) and extending the representation of multiphase chemistry, which started with Rosanka et al. (2020), to deliquescent aerosols.

> *I also feel this will help focus the paper as currently it reads as one in which aromatics vs no-aromatics is the focus, but given we know aromatics are important (and abundant in urban environments) shouldn't the focus be Arom vs OnlyMCM? At least I find this comparison more interesting than Arom vs NoArom.It would be good if there were some figures (perhaps in an appendix) which compare the OnlyMCM and Arom scheme under idealised (Box model) conditions. Ideally this would be against laboratory data but I think even against some general scenarios it would be very useful to see how the differences implemented affect the results and then some sensitivity analysis could be performed I think quite straightforwardly to look at the impacts of some of these uncertain thermal-kinetic and photolytic processes.*

Reply:
We thank the referee for this comment. Currently, we are not setup to compare box model simulations to lab data from chamber experiments. Our *modus operandi* is to obtain an intermediate and faithful reduction of a chemical mechanism like MCM that has been widely used and tested against lab measurements. We also believe that the differences in the results between AROM and onlyMCM are interesting to show. Instead of showing box model simulation results under idealized conditions, we think that showing the global distribution of the differences (spanning many possible scenarios) between AROM and onlyMCM simulations is a synthetic and useful way to visualize the deviations across a comprehensive set of chemical regimes. We therefore added an appendix to the manuscript to enhance the discussion of the differences between the MCM mechanism and our mechanism for the aromatics. In this appendix we briefly present the differences for the main oxidants OH, O_3 and NO_3.

The text of the appendix is reported below

In this appendix the impact of the modifications to the MCM chemistry (listed in Sect. 2) on the model results are shown for the main atmospheric oxidants.

Hydroxyl radical (OH)

The differences at the surface are shown in Figure A1. Much of the increase in Figure 3 can be ascribed to the enhanced HO_x production by photolysis of benzaldehyde (Roth et al., 2010) and HONO from R1. The latter from benzene chemistry explains the significant enhancement across the UT/LS (see Fig. A2).

Ozone (O_3)

The differences at the surface are shown in Figure A3. It can be seen that lareg part of the enhancement in surface ozone mixing ratio in Figure 6 is due to enhanced HO_x production in regions that are not NO_x-limited. The zonal mean change in ozone is minimal and slightly positive at the tropical UT/LS (Fig. A5).

Nitrate radical (NO_3)

The differences at the surface are shown in Figure A5. It can be seen that the widespread enhancement of in Figure 12 is largely to be ascribed to the effect of phenylperoxy reaction with NO_2 (R2).

> ***Specific Comments***
>
> *L13: Changes of what?*

Reply:
We added "of trace gas levels" to the text.

> *L19: Is this a net loss? If not, is it a very important finding?*

Reply:
This is a direct loss of ozone. As it is localized in the upper troposphere where benzene is transported and NO levels are generally low, this turns into a net loss of ozone. However, model setup used in this study did not have a comprehensive set of passive tracers that allows the classical tropospheric O_x budget to be computed. Nevertheless, we think that this result, the direct loss of ozone, is worth noting especially because it is clearly missing in all other global models with which the global impact of aromatics on ozone has been estimated to be positive, contrary to our study.

> *L31: This is too vague. There are specific definitions of aromaticity with implications for the chemistry of compounds in this class.*

Reply:
We agree with the referee that we need to be more specific in this respect. Thus, we have changed the first sentence of the paragraph by stating that aromatics are unsaturated planar cyclic organic compounds with enhanced stability due to a strong electron delocalization.

We have modified the text

Aromatics are a subset of unsaturated organic compounds of which several are present in the atmosphere, e.g., benzene, toluene, ethylbenzene, xylenes, styrene and trimethylbenzenes.

to

Aromatics are unsaturated planar cyclic organic compounds with enhanced stability due to a strong electron delocalization. Several of them are present in the atmosphere, e.g., benzene, toluene, ethylbenzene, xylenes, styrene and trimethylbenzenes.

> *L38: Add a reference for the toluene biogenic emissions.*

Reply:
We added the reference to the first reported biogenic emission of toluene by Heiden et al. (1999).

> *L42: Is that true of all aromatics? i.e. benzene?*

Reply:
We agree with the referee that it might sound odd to put benzene in the category of organic compounds that have a high reactivity. We have changed the relative sentence by removing the reference to the high reactivity and expressed in more neutral terms with a range of tropospheric lifetimes.

Accordingly, we have modified the sentence

Due to their high reactivities, aromatics have relatively short atmospheric lifetimes ranging from hours to a few days.

with

Aromatics have relatively atmospheric lifetimes ranging from a few hours, e.g. for trimethylbenzene, to about ten days, e.g. for benzene (Atkinson and Arey, 2003).

> *L46-50: There is a rich literature on many aspects of this chemistry which should be cited.*

Reply:
We agree with the referee and we added the references to the review papers by Atkinson and Arey (2003) and Vereecken (2019). For the SOA formation from aromatics oxidation we now refer to Henze et al. (2008) and Lin et al. (2012).

> *L78: How were they added? i.e. what cross-sections and quantum yields used?*

Reply:
We apologize for the lack of detail here. For the photolytic HONO-formation from nitrophenols the cross sections and quantum yield provided by Chen et al. (2011) are used by the JVAL and JVPP models (Sander et al., 2014) for calculating the j-values. We have modified the manuscript accordingly.

In JVAL (Sander et al., 2014) the cross sections for 2-nitrophenol and 3-methyl-2-nitrophenol and the quantum yield for 2-nitrophenol by Chen et al. (2011) are used to calculate the j-values.

> *L89: Please be quantitative.*

Reply:
We have added to the revised manuscript the information on the yields of glyoxal (60%) and methylglyoxal (40%) for toluene from Birdsall et al. (2010). We also specify now that these yields are for the non-radical terminating channels in the reactions with NO and HO_2.

We have replaced the text

Bicyclic peroxy radicals in the oxidation mechanism of toluene produce some glyoxal and methyl glyoxal as suggested by Birdsall et al. (2010). Benzene is treated analogously.

with

Bicyclic peroxy radicals in the oxidation mechanism of toluene yield 60% glyoxal and 40% methyl glyoxal from the non-radical terminating reactions with NO and HO_2 as suggested by Birdsall et al. (2010). Benzene is treated analogously but yields 100% glyoxal from the above mentioned reactions.

> *L110: Please plot the data in nmol/mol to make things clearer for the reader.*

Reply:
Yes, we now plot the data with mol/mol and the appropriate exponent for the range of values shown. We agree it was not clear before.

> *L118: Insert "surface" between these two words.*

Reply:
Done.

> *L131-132: Can you be more specific on both the impact on the OH NH:SH ratio change and the impact on the methane lifetime.*

Reply:
Referee #1 had a similar comment and we acknowledge that the quantification of the impact on methane lifetime could have been given more space than a short mention without referring to Table 4. Therefore, we have extended the paragraph L129-132 by pointing explicitly to Table 4 and shortly discussing the changes in OH and CH4 lifetime in the two hemispheres.

The paragraph

Figure 5 shows the annual zonal mean changes of the OH mixing ratio. The changes are most pronounced in the NH upper troposphere where reductions range from 7 % to 20 %. This helps bringing the model-simulated inter-hemispheric OH asymmetry closer to that derived from observations (?). Globally, aromatics oxidation reduces OH by 7.7 % and consequently increases methane lifetime.

has been extended:

Figure 5 shows the annual zonal mean changes of the OH mixing ratio. The changes are most pronounced in the NH upper troposphere where reductions range from 7 % to 20 %. These predicted changes are associated to similar reductions in NO_x. In fact, the upper troposphere is in general NO_x-limited and the oxidation of aromatics enhances the formation N_2O_5 and HNO_3 which are lost heterogeneously. This leads to an effective removal of NO_x from the gas phase and lowers the radical production. The change in hemispheric burdens of OH are consistent with this picture (Table 4). This moderately helps bringing the model-simulated inter-hemispheric OH asymmetry closer to that derived from observations (?). Globally, aromatics oxidation reduces OH by 7.7 % and consequently increases methane lifetime by about 5.5 %. The changes are more pronounced in the northern hemisphere where aromatics are mostly emitted (Table 4). However, the latter in the EMAC model remains significantly lower than the ACCMIP multi-model mean and the observational-based estimates (?). Coarse model spatial resolutions (about 200 km) are known to result in an overestimation (underestimation) of global mean OH (methane lifetime) of at least 5 % (?). This is due to a less efficient conversion of NO_x to NO_y when strong pollutant emissions are artificially diluted in the model grid boxes. This aspect certainly has a larger impact on the inter-hemispheric OH asymmetry in atmospheric models that is in contrast to observational estimates (?).

> *L135-136: Has there been an increase in the flux through O3+OH? I'm surprised given the OH has gone down in these regions.*

Reply:
We thank the referee for spotting this inconsistency. Clearly, the simulation results do not support the statement on an increase in the flux of the O_3 + OH reaction in ozone-depleting regimes, e.g. over the ocean. We have removed OH from this explanation.

> *L141: Odd to ref. Fig 9 before 7 or 8. Re-order?*

Reply:
Thank you for spotting this. The figures are reordered now.

> *L153: Can you confirm which definition you used in the analysis?*

Reply:
We put this text in the caption of Table 4.

Tropospheric burdens were reckoned using six different tropopause definitions (provided by the TROPOP submodel, see Jöckel et al. (2010) for details): 1,2) surfaces of O_3 mixing ratio of 125 and 150 nmol/mol, respectively, 3) WMO definition (WMO (1957)), 4) dynamic PV-based (3.5 PVU potential vorticity surface, sought within 50–800 hPa), 5) climatological (invariable zonal profile, i.e. $300\text{-}215\times(\cos(\text{latitude}))^2$ hPa) and 6) the combined definition (WMO tropopause within 30°N–30°S, otherwise dynamic PV-based tropopause). The latter definition is used by default in EMAC and in this manuscript to report tropospheric budgets. Estimated changes to tropospheric O_3 burden are identical within 0.05% between the available definitions, which we conclude as robust against the definition used.

> *L155: Is it widely acknowledged that it is "only" ozonolysis? And does the definition of loss change with different constructs of the O3 budget (c.f. Bates and Jacob 2019)?*

Reply:
According to the expanded definition of the odd oxygen budget by Bates and Jacob (2020), the loss ozone from reaction with phenoxy radical would count as half since RO_2 formation is counted with the "stoichiometric" coefficient 0.5 in the O_y family. This coefficient is justified in order to account for the effect the $O(^1D) + H_2O$ reaction has on OH. However, the rationale and validity of this "stoichiometric" accounting for peroxy radicals is not clear. We agree that when ozone reacts with phenoxy radical close to the pollution sources the NO-to-NO_2 conversion by the resulting phenyl peroxy radical would largely compensate the ozone loss in question. However, in the upper troposphere where benzene is transported and where NO levels are usually low, the loss of ozone with phenoxy is a net loss.

> *L156: Perhaps add e.g., as this is just one models calculation.*

Reply:
Done.

> *L161: Confirm if you mean ozone or odd-oxygen?*

Reply:
We mean ozone.

> *L166-167: Can you quantify the relative contribution of these different pathways to the 200 Tg/yr O3 (odd oxygen?) loss?*

Reply:
We now realize that our formulations have been not clear and misleading. The 200-300 Tg/yr we give in the manuscript is the direct ozone loss in the reaction with (substituted) phenoxy radicals. What we wanted to express here was that the phenyl peroxy radical produced by reaction R3 enhances the NO_3 formation at night, which in turn enhances the O_x via the heterogeneous loss of N_2O_5. Having no detailed passive tracers for computing the O_x budget in this study, we cannot quantify the strength of the O_x destruction we describe. We now make this clearer in the revised manuscript.

> *L174: But the way you have written R1 suggests that phenoxy radicals are not formed (instead butenedial is formed).*

Reply:
Indeed R1 destroys the aromaticity of the molecule and therefore any possibility to form further (substituted) phenoxy radicals. Unfortunately, we have not explicitly mentioned that in MCM (AROM and onlyMCM simulations) the reactions of the simplest nitrophenol (HOC6H4NO2) yield a nitrophenoxy radical which is assumed to react with O_3 and NO_2 like phenoxy radical (C6H5O). We have made this point clearer in the revised manuscript.

> *Table 3: Can you confirm that these are area weighted? The surface ozone seems a bit high compared to other models I've seen.*

Reply:
Yes, they are. We have added this information in the table caption. We share the impression of the reviewer that the model computes high levels of surface ozone. We are addressing the general overestimation of tropospheric ozone by, among others, improvements of the dry deposition scheme lacking the non-stomatal sink (Emmerichs et al., 2020) and the explicit modelling of the ozone sink in cloud droplets (Rosanka et al., 2020) and deliquescent aerosols.

References

Atkinson, R. and Arey, J.: Atmospheric degradation of volatile organic compounds, Chem. Rev., 103, 4605–4638, https://doi.org/10.1021/cr0206420, 2003.

Bates, K. H. and Jacob, D. J.: An Expanded Definition of the Odd Oxygen Family for Tropospheric Ozone Budgets: Implications for Ozone Lifetime and Stratospheric Influence, Geophysical Research Letters, 47, e2019GL084 486, https://doi.org/https://doi.org/10.1029/2019GL084486, URL `https://agupubs.onlinelibrary.wiley.com/doi/abs/10.1029/2019GL084486`, e2019GL084486 10.1029/2019GL084486, 2020.

Birdsall, A. W., Andreoni, J. F., and Elrod, M. J.: Investigation of the role of bicyclic peroxy radicals in the oxidation mechanism of toluene, J. Phys. Chem. A, 114, 10 655–10 663, https://doi.org/10.1021/jp105467e, 2010.

Chen, J., Wenger, J. C., and Venables, D. S.: Near-ultraviolet absorption cross sections of nitrophenols and their potential influence on tropospheric oxidation capacity, J. Phys. Chem. A, 115, 12 235–12 242, https://doi.org/10.1021/jp206929r, 2011.

Emmerichs, T., Kerkweg, A., Ouwersloot, H., Fares, S., Mammarella, I., and Taraborrelli, D.: A revised dry deposition scheme for land-atmosphere exchange of trace gases in ECHAM/MESSy v2.54, Geoscientific Model Development Discussions, 2020, 1–32, https://doi.org/10.5194/gmd-2020-139, URL `https://gmd.copernicus.org/preprints/gmd-2020-139/`, 2020.

Heiden, A. C., Kobel, K., Komenda, M., Koppmann, R., Shao, M., and Wildt, J.: Toluene emissions from plants, Geophysical Research Letters, 26, 1283–1286, https://doi.org/https://doi.org/10.1029/1999GL900220, URL `https://agupubs.onlinelibrary.wiley.com/doi/abs/10.1029/1999GL900220`, 1999.

Henze, D., Seinfeld, J., Ng, N., Kroll, J., Fu, T.-M., Jacob, D. J., and Heald, C.: Global modeling of secondary organic aerosol formation from aromatic hydrocarbons: high-vs. low-yield pathways, Atmos. Chem. Phys., 8, 2405–2420, 2008.

Jöckel, P., Kerkweg, A., Pozzer, A., Sander, R., Tost, H., Riede, H., Baumgaertner, A., Gromov, S., and Kern, B.: Development cycle 2 of the Modular Earth Submodel System (MESSy2), Geosci. Model Dev., 3, 717–752, https://doi.org/10.5194/GMD-3-717-2010, 2010.

Lin, G., Penner, J. E., Sillman, S., Taraborrelli, D., and Lelieveld, J.: Global modeling of SOA formation from dicarbonyls, epoxides, organic nitrates and peroxides, Atmos. Chem. Phys., 12, 4743–4774, https://doi.org/10.5194/acp-12-4743-2012, 2012.

Rosanka, S., Sander, R., Franco, B., Wespes, C., Wahner, A., and Taraborrelli, D.: Oxidation of low-molecular weight organic compounds in cloud droplets: global impact on tropospheric oxidants, Atmospheric Chemistry and Physics Discussions, 2020, 1–33, https://doi.org/10.5194/acp-2020-1041, URL `https://acp.copernicus.org/preprints/acp-2020-1041/`, 2020.

Roth, E., Chakir, A., and Ferhati, A.: Study of a benzoylperoxy radical in the gas phase: ultraviolet spectrum and $C_6H_5C(O)O_2 + HO_2$ reaction between 295 and 357 K, J. Phys. Chem. A, 114, 10 367–10 379, https://doi.org/10.1021/jp1021467, 2010.

Sander, R., Jöckel, P., Kirner, O., Kunert, A. T., Landgraf, J., and Pozzer, A.: The photolysis module JVAL-14, compatible with the MESSy standard, and the JVal PreProcessor (JVPP), Geosci. Model Dev., 7, 2653–2662, https://doi.org/10.5194/GMD-7-2653-2014, 2014.

Vereecken, L.: Reaction Mechanisms for the Atmospheric Oxidation of Monocyclic Aromatic Compounds, chap. Chapter 6, pp. 377–527, World Scientific Publishing, https://doi.org/10.1142/9789813271838_0006, URL `https://www.worldscientific.com/doi/abs/10.1142/9789813271838_0006`, 2019.

WMO: Definition of the tropopause and of significant levels, URL `https://library.wmo.int/doc_num.php?explnum_id=6960`, 1957.

Influence of aromatics on tropospheric gas-phase composition

Domenico Taraborrelli[1], David Cabrera-Perez[2], Sara Bacer[2,*], Sergey Gromov[2], Jos Lelieveld[2], Rolf Sander[2], and Andrea Pozzer[2,3]

[1]Institute of Energy and Climate Research (IEK-8), Forschungszentrum Jülich GmbH, 52425 Jülich, Germany
[2]Atmospheric Chemistry Department, Max-Planck Institute of Chemistry, Hahn-Meitner-Weg 1, 55128 Mainz, Germany
[3]International Centre for Theoretical Physics, 34100 Trieste, Italy
[*]Now at: Université Grenoble Alpes, CNRS, Grenoble INP, LEGI, 38000 Grenoble, France

Correspondence: D. Taraborrelli (d.taraborrelli@fz-juelich.de)

Abstract.

Aromatics contribute a significant fraction to organic compounds in the troposphere and are mainly emitted by anthropogenic activities and biomass burning. Their oxidation in lab experiments is known to lead to the formation of ozone and aerosol precursors. However, their overall impact on tropospheric composition is uncertain as it depends on transport, multiphase chemistry, and removal processes of the oxidation intermediates. Representation of aromatics in global atmospheric models has been either neglected or highly simplified. Here, we present an assessment of their impact on the gas-phase chemistry, using the general circulation model EMAC (ECHAM5/MESSy Atmospheric Chemistry). We employ a comprehensive kinetic model to represent the oxidation of the following monocyclic aromatics: benzene, toluene, xylenes, phenol, styrene, ethylbenzene, trimethylbenzenes, benzaldehyde, and lumped higher aromatics that contain more than 9 C atoms.

Significant regional changes are identified for several species. For instance, glyoxal increases by 130 % in Europe and 260 % in East Asia, respectively. Large increases in HCHO are also predicted in these regions. In general, the influence of aromatics is particularly evident in areas with high concentrations of NO_x, with increases up to 12 % in O_3 and 17 % in OH.

On a global scale, the estimated net changes of trace gas levels are minor when aromatic compounds are included in our model. For instance, the tropospheric burden of CO increases by about 6 %, while the burdens of OH, O_3, and NO_x (NO + NO_2) decrease between 3 % and 9 %. The global mean changes are small, partially because of compensating effects between high- and low-NO_x regions. The largest change is predicted for the important aerosol precursor glyoxal, which increases globally by 36 %. In contrast to other studies, the net change in tropospheric ozone is predicted to be negative, -3 % globally. This change is larger in the northern hemisphere where global models usually show positive biases. We find that the reaction with phenoxy radicals is a significant loss for ozone, of the order of 200-300 $\mathrm{Tg/yr}$, which is similar to the estimated ozone loss due to bromine chemistry.

Although the net global impact of aromatics is limited, our results indicate that aromatics can strongly influence tropospheric chemistry on a regional scale, most significantly in East Asia. An analysis of the main model uncertainties related to oxidation and emissions suggests that the impact of aromatics may even be significantly larger.

1 Introduction

Volatile organic compounds (VOCs) comprise a large variety of species which influence the tropospheric chemistry at local, regional, and global scales. VOCs react mainly with the hydroxyl radical (OH), ozone (O_3), and the nitrate radical (NO_3), or they are photolyzed. Their oxidation affects many key atmospheric species, including OH, O_3, and nitrogen oxides (NO_x = NO + NO_2). Production and destruction of ozone ~~are~~ is controlled by the ratio of VOCs to NO_x. In the low-NO_x regime, the net effect of VOC oxidation is ozone destruction. Under high-NO_x conditions, e.g., in urban areas, O_3 is generated by the oxidation of VOCs (Sillman et al., 1990).

Aromatics are ~~a subset of unsaturated organic compounds of which several~~ unsaturated planar cyclic organic compounds with enhanced stability due to a strong electron delocalization. Several of them are present in the atmosphere, e.g., benzene, toluene, ethylbenzene, xylenes, styrene and trimethylbenzenes. In general, aromatic compounds are found in continental areas, especially in industrialized urban and semi-urban regions (Barletta et al., 2005) where their emissions are highest. They are responsible for a considerable fraction of ozone and secondary organic aerosol (SOA) formation (Ng et al., 2007; Lee et al., 2002; Ran et al., 2009). In addition, many aromatics are toxic (WMO, 2000).

Emissions of aromatics are primarily anthropogenic, related to fuel combustion, and leakage from fuels and solvents (Koppmann, 2007; Sack et al., 1992). Emissions from biomass burning play a secondary role but can be important on a regional scale (Cabrera-Perez et al., 2016). Biogenic emissions are only relevant for toluene (Heiden et al., 1999), although recent studies suggest that other aromatics from biogenic sources may rival those from fossil fuel use (Misztal et al., 2015).

As shown by Cabrera-Perez et al. (2016), aromatic compounds are removed from the atmosphere mainly via chemical oxidation. Dry deposition is a minor sink, and wet deposition is almost negligible. The gas-phase chemistry of aromatics has been the subject of many studies (e.g., Atkinson et al., 1989; Warneck, 1999; Koppmann, 2007). ~~Due to their high reactivities, aromatics have relatively short~~ Aromatics have relatively atmospheric lifetimes ranging from ~~hours to a few days.~~ a few hours, e.g. for trimethylbenzene, to about ten days, e.g. for benzene (Atkinson and Arey, 2003). Their oxidation is mainly controlled by the OH radical but they also react with NO_3 and O_3. The reaction with OH can proceed along two principal pathways. The first starts with H-abstraction from an aliphatic substituent. The following reactions are similar to those of aliphatic compounds and involve the addition of O_2, yielding a peroxy radical as an intermediate. Toluene, for example, can be oxidized in this way to benzaldehyde (Atkinson and Arey, 2003, and references therein). The second, which is the dominant path, is OH addition to the aromatic ring. Secondary reactions can lead to ring opening and complex further reactions, eventually generating HCHO, glyoxal, and other smaller organic molecules (Vereecken, 2019, and references therein). The products from the oxidation of aromatic compounds have a reduced volatility and allow for the formation of SOA (Henze et al., 2008; Lin et al., 2012), which in turn can significantly reduce the gas-phase concentrations of the aromatic oxidation products.

Numerical models are essential to understand the highly complex chemical degradation of aromatics and to quantify the impact of these compounds in atmospheric chemistry. A very detailed modeling of aromatics is possible with the reactions contained in the Master Chemical Mechanism (MCM, Jenkin et al., 2003). However, due to its complexity, the full mechanism is mainly suitable for box model calculations. For global studies, simplified reaction schemes are usually used (e.g., Emmons et al., 2010; Hu et al., 2015).

The main objective of this study is to investigate how tropospheric OH, O_3, NO_x, and several VOC concentrations are affected by the oxidation of several monocyclic aromatics. The paper is organized as follows. In Sect. 2, the numerical model and the set-up of the simulations are described. Section 3 analyzes the calculated impact on selected chemical species both on the global and on the regional scales.

2 Model description

We used the ECHAM5/MESSy Atmospheric Chemistry (EMAC) model, which is a numerical chemistry and climate simulation system that includes submodels describing tropospheric and middle atmosphere processes (Jöckel et al., 2010). EMAC uses the second version of the Modular Earth Submodel System (MESSy2) to link multi-institutional computer codes. The core atmospheric model is the 5th generation European Centre Hamburg general circulation model (ECHAM5, Roeckner et al., 2006).

For the present study we performed simulations with EMAC (ECHAM5 version 5.3.02, MESSy version 2.53) in the T63L31ECMWF resolution, which corresponds to a grid with a horizontal cell size of approximately $1.875° \times 1.875°$ and 31 vertical hybrid pressure levels, extending from the surface up to about 10 hPa.

Emission rates of the individual aromatics are shown in ~~Tab.~~Table 1. The sum of all sources is 29.4 $\mathrm{TgC/a}$. For anthropogenic emissions, we used EDGAR 4.3.2 (Huang et al., 2017), distributed vertically as in Pozzer et al. (2009). The MESSy submodel MEGAN calculates biogenic emissions (Guenther et al., 2012). For biomass burning, the submodel BIOBURN was used, which integrates the Global Fire Assimilation System (GFAS) inventory (Kaiser et al., 2012).

Atmospheric chemistry was calculated with the MECCA submodel, which has been evaluated by Pozzer et al. (2007) and Pozzer et al. (2010). The most recent model version has been described by Sander et al. (2019). The mechanism for aromatic species is a reduced version of the MCM (Bloss et al., 2005b), as described in detail by Cabrera-Perez et al. (2016). In ~~this~~ short, the MCM schemes for benzene and toluene were taken. Following the approach of Taraborrelli et al. (2009), short-lived intermediates were replaced with their stable products and isomeric peroxy radicals were lumped preserving the yield of stable products. Initial oxidation steps of aromatics other than benzene and toluene are considered and products replaced by the analogous toluene oxidation products. This approximation inherently introduces an error with respect to the formation of larger and low volatile products. The carbon mass that is not accounted for with this approximation is however tracked by introducing the counter LCARBON for the difference of carbon atoms between the oxidation products of larger aromatics and toluene. In this study, we consider several additions to the MCM reactions:

- For several nitrophenols (MCM names: HOC6H4NO2, DNPHEN, TOL1OHNO2, MNCATECH, DNCRES), their ~~photolysis reactions~~ photolytic production of HONO were added (Bejan et al., 2006), e.g.:

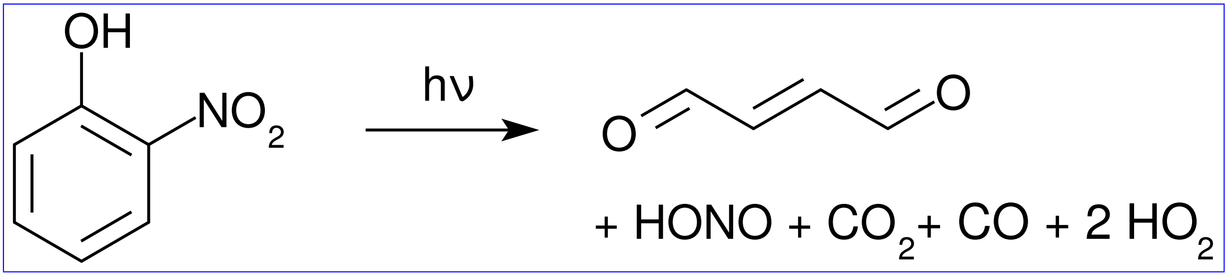

(R1)

In JVAL (Sander et al., 2014) the cross sections for 2-nitrophenol and 3-methyl-2-nitrophenol and the quantum yield for 2-nitrophenol by Chen et al. (2011) are used to calculate the j-values.

- For the photolysis of benzaldehyde, the MCM uses the rate constant (j-value) of methacrolein as a proxy. ~~We have calculated~~ Our model calculates with JVAL (Sander et al., 2014) the j-value based on the UV/VIS spectrum of benzaldehyde recommended by Wallington et al. (2018). In our code, the photolysis of benzaldehyde produces $C_6H_5O_2$, HO_2 and CO.

- For several phenyl peroxy compounds (MCM names: C6H5O2, CATEC1O2, OXYL1O2, MCATEC1O2, NCRES1O2), their reactions with NO_2 were added (Jagiella and Zabel, 2007), e.g.:

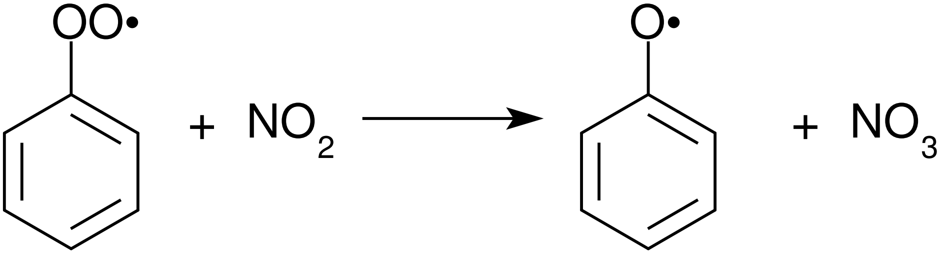

(R2)

- For the reaction of HO_2 with the peroxy radical C6H5CO3 (resulting from the oxidation of benzaldehyde), we use the yields provided by Roth et al. (2010).

- Alkyl nitrate yields are calculated as a function of temperature and pressure, as described by Sander et al. (2019).

- Bicyclic peroxy radicals in the oxidation mechanism of toluene ~~produce some glyoxal and methyl glyoxal~~ yield 60% glyoxal and 40% methyl glyoxal from the non-radical terminating reactions with chemNO and HO_2 as suggested by Birdsall et al. (2010). Benzene is treated analogously but yields 100% glyoxal from the above mentioned reactions.

The aerosol calculations follow the approach of Pringle et al. (2010), with the notable difference of the inclusion of the explicit organic aerosol submodel ORACLEv1.0 by Tsimpidi et al. (2014). Although, similar to Tsimpidi et al. (2014), low-and intermediate volatiles are parameterized as lumped species, the equilibrium with their equivalent aerosol phase is explicitly calculated for $\simeq$ 600 volatile organic carbon tracers via ORACLE. The volatility and the enthalpy of vaporization of each tracer is estimated with the approaches of Li et al. (2016) and Epstein et al. (2010), respectively.

The simulated period covers the years 2009–2010, with the first year as spin-up, and the year 2010 being used for the analysis. The feedback between radiation and chemistry was decoupled to avoid any influence of chemistry on the dynamics (QCTM mode by Deckert et al. (2011)). As a consequence, every simulation discussed here has the same meteorology, i.e., binary identical transport.

To analyze the influence of the aromatic compounds on atmospheric chemistry and composition, we performed three model simulations, as listed in ~~Tab.~~Table 2. The *AROM* simulation includes all chemical reactions and emissions of the following monocyclic aromatic compounds: benzene, toluene, xylenes (lumped), phenol, styrene, ethylbenzene, trimethylbenzenes (lumped), benzaldehydes, and higher aromatics (as representative of aromatics with more than 9 carbon atoms). The reference simulation (*NOAROM*) is identical to *AROM*, except that it excludes aromatic compounds. In the *ONLYMCM* run, we reverted the additions and changes to the MCM that have been described above. Our focus is to compare *AROM* with *NOAROM*. Results of *ONLYMCM* are mainly interesting for benzaldehyde and HONO. As EMAC uses terrain-following vertical hybrid pressure coordinates, we will refer to “surface” as the lowest model level, with an average thickness of roughly 60 m.

3 Results and discussion

Globally averaged surface mixing ratios obtained from all model simulations (*AROM*, *NOAROM*, and *ONLYMCM*) are listed in ~~Tab.~~Table 3. Figure 1 shows the annual average mixing ratios of the sum of all aromatic compounds included in the simulation *AROM*. They are higher in continental areas and close to the surface. The highest values are predicted in the northern hemisphere (NH), in particular, in East and South Asia, as well as in parts of Europe, Africa, and the US, reaching up to about $1\ \mathrm{nmol/mol}$. The background mean mixing ratios in oceanic areas of the southern hemisphere (SH) are of the order of a few $\mathrm{pmol/mol}$. For a more detailed analysis, we have selected the following five regions, as defined in Figure 2: Amazon area (AMA), central Africa (CAF), eastern Asia (EAS), Europe (EUR), and eastern US (EUS). The budgets of selected chemical species were calculated within these regions (~~Tab.~~Table 5).

3.1 Hydroxyl radical (OH)

Figure 3 shows the model-calculated surface OH in the *AROM* and *NOAROM* simulations. When aromatics are introduced to the model, the global average concentration of OH decreases for two reasons: first, the direct reaction with aromatics consumes OH, and second, additional CO resulting from the degradation of aromatics represents an increased sink for OH. However, in eastern Asia, Europe, and the east coast of the US, where NO_x concentrations are high, an increase of OH can be seen. Although the aromatics decrease NO_x in these areas (see below), the chemical system remains in the high-NO_x regime.

~~We find a positive correlation between~~ We find that inclusion of aromatics emissions leads to an increase OH ~~and anthropogenic emissions~~ in these regions but ~~a negative correlation~~ to decrease in the low-NO_x CAF region. The increased OH in the high-

NO_x regions is mainly caused by the reaction of NO with HO_2. The production of OH from this important reaction is enhanced by the significant HO_2 formation in aromatics oxidation. Compared to *onlyMCM* the *AROM* simulation has additional HO_2 production from the photolysis of ortho-nitrophenols (R1) and benzaldehyde (Sect. 2). The enhanced HO_2 levels (not shown) overcompensates the negative changes in NO (see Sect. 3.3).

Figure 4 shows the seasonal cycle of the OH mixing ratio in the planetary boundary layer for the NH and SH. Inclusion of the aromatics leads to a relative decrease between 2.5 % and 5.5 %. Higher OH concentrations are identified over continental areas during the NH autumn, winter and spring than in summer (Fig. 3). In summer, OH concentrations increase only at a few locations when aromatics are included. In general enhancements are predicted for regions where radical production is not NO_x-limited. In the NH there obviously more such regions compared to the SH. However, the largest decrease in the planetary boundary OH is computed for the NH where most of the emissions of aromatics are located.

Figure 5 shows the annual zonal mean changes of the OH mixing ratio. The changes are most pronounced in the NH upper troposphere where reductions range from 7 % to 20 %. ~~This~~ These predicted changes are associated to similar reductions in NO_x. In fact, the upper troposphere is in general NO_x-limited and the oxidation of aromatics enhances the formation N_2O_5 and HNO_3 which are lost heterogeneously. This leads to an effective removal of NO_x from the gas phase and lowers the radical production. The change in hemispheric burdens of OH are consistent with this picture (Table 4). This moderately helps bringing the model-simulated inter-hemispheric OH asymmetry closer to that derived from observations (Lelieveld et al., 2016). Globally, aromatics oxidation reduces OH by 7.7 % and consequently increases methane lifetime ~~.~~ by about 5.5 %. The changes are more pronounced in the northern hemisphere where aromatics are mostly emitted (Table 4). However, the latter in the EMAC model remains significantly lower than the ACCMIP multi-model mean and the observational-based estimates (Naik et al., 2013). Coarse model spatial resolutions (about 200 km) are known to result in an overestimation (underestimation) of global mean OH (methane lifetime) of at least 5 % (Yan et al., 2016). This is due to a less efficient conversion of NO_x to NO_y when strong pollutant emissions are artificially diluted in the model grid boxes. This aspect certainly has a larger impact on the inter-hemispheric OH asymmetry in atmospheric models that is in contrast to observational estimates (Patra et al., 2014) .

Differences for OH between the *AROM* and *onlyMCM* simulations are shown in Figures A1 and A2 of the Appendix A.

3.2 Ozone (O_3)

In most areas of the globe, surface ozone is slightly lower in *AROM* than in *NOAROM* (Fig. 6). The O_3 reduction is due to (i) the decrease in NO_x concentrations (limiting ozone formation) and (ii) increasing radical production (~~, ,~~ HO_x, and RO_2) in ozone-depleting regimes, which enhances ~~reactions~~ reaction of O_3 with HO_2~~and~~. Only a few high-NO_x regions, where hydrocarbons are the limiting factor for ozone formation, show increased ozone concentrations: mainly East China (EAS), but also the eastern US (EUS) and Europe (EUR). The increases in these areas ~~correlate~~ is associated with anthropogenic emissions of aromatics, which have significant ozone formation potentials. We find ~~a positive correlation between~~ that anthropogenic emissions of aromatics leads to an increase of O_3 ~~and anthropogenic emissions~~ in the EAS and EUR regions but ~~a negative correlation~~ to a decrease in the low-NO_x CAF region.

The seasonal cycles of the relative differences show lower amplitude than for OH, but similar patterns (Fig. 7). The impact of aromatics is smallest in summer. Like for the OH levels, the inter-hemispheric asymmetry in the emission of aromatics determines the higherO_3 decrease in the NH compared to the SH.

The zonal mean changes of O_3 mixing ratio in the troposphere are uniformly negative (Fig. 8). Similar to surface ozone, the annual mean changes for *ONLYMCM* and *AROM* are $-2.3\,\%$ and $-3.0\,\%$, respectively. The hemispheric changes are shown in ~~Tab.~~Table 4. It is well known that MCM for aromatics overestimates ozone production in chamber experiments (Bloss et al., 2005b). The issue has been analysed in the companion paper (Bloss et al., 2005a) where the best mechanism improvement was found to be an early OH source during oxidation. Cabrera-Perez et al. (2016) introduced enhanced HO_x-sources by photolysis of benzaldehyde and nitrophenols. These modifications consistently result in less ozone produced with respect to MCM. These results deviate from the results by Yan et al. (2019) who suggested a global increase of 0.4 % due to aromatics. However, they only considered benzene, toluene and xylenes. Our results, obtained with a more comprehensive setup, suggest that aromatics could slightly ameliorate the model overestimate in the NH (Jöckel et al., 2016; Young et al., 2018). The overall tropospheric ozone burden decreases from 381 to 369 Tg for the *AROM* simulation. These estimated changes are robust against the tropopause definition and are about -3.5 and -2.3 % for the Northern and Southern Hemispheres, respectively (Table 4).~~These changes are associated with the enhanced~~

The changes in ozone are caused by perturbations of the radical production in different NO_x regimes but also by the direct ozone loss ~~by~~ in reactions with organic compounds. It is widely acknowledged that this direct loss is only due to the ozonolysis of unsaturated VOCs and is estimated to be about 100 $\mathrm{Tg/yr}$, less than 2 % of the tropospheric ozone budget ~~(Tilmes et al., 2016)~~ ~~.~~(e.g. in Tilmes et al. (2016)). However, with aromatics a new direct ozone loss process involving organic radicals comes in place. In Figure 9 the change in tropospheric ozone burden is shown against the change in ozone loss with organic compounds. This change is estimated to be globally in the 200-300 Tg/yr range depending on the mechanism used and is comparable to the loss by bromine chemistry in the troposphere (Sherwen et al., 2016)~~)~~. Ozone is known to react with organic radicals like methyl peroxy radical although this loss is an insignificant sink (Tyndall et al., 1998). We find that (substituted) phenoxy radicals from aromatics are a significant sink term of ozone (>200 $\mathrm{Tg/yr}$). These radicals are unique to aromatics oxidation and they also react with NO and NO_2. When the concentrations of NO_x are relatively low, C_6H_5O has sufficiently long lifetime to react with O_3. This ozone loss is modelled based on the results by Tao and Li (1999) for phenoxy radical

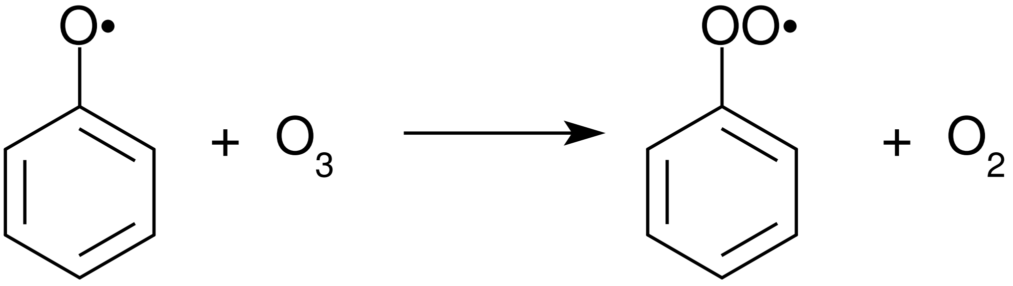

(R3)

~~This ozone loss~~ Although the know rate constant for reaction R3 is about one order of magnitude lower than the others, the high abundance in the atmosphere makes ozone the major sink of (substituted) phenoxy radicals. This direct ozone loss in reaction R3 is enhanced by phenoxy radical production in ~~the R2 reaction and the subsequent~~ reaction R2 and the concurrent loss of odd oxygen by NO_3 photolysis and N_2O_5 heterogeneous loss

$$\mathrm{NO_3 + h\nu} \rightarrow \mathrm{NO + O_2} \tag{R4}$$

$$\mathrm{NO_3 + NO_2} \rightarrow \mathrm{N_2O_5} \tag{R5}$$

$$\mathrm{N_2O_5 + H_2O} \rightarrow \mathrm{2HNO_3(aq)} \tag{R6}$$

In our chemical kinetics mechanism (also in MCM) the reaction system just described constitutes an effective catalytic destruction cycle of odd oxygen. The strength of this cycle has not been diagnosed in this study. Nevertheless, we observe that it depends on the (substituted) phenoxy radical levels and is significantly reduced in *AROM* compared to *onlyMCM* (Figure 9). We ascribe this difference to MCM not accounting for the photolysis of nitrophenols (R1) as determined by Bejan et al. (2006)~~preventing reformation of phenoxy radicals.~~. In fact, in MCM the first nitrophenols from benzene (HOC6H4NO2) and toluene (TOL1OHNO2) solely form nitrophenoxy radicals with the same reactivity of the unsubstituted phenoxy radical (C6H5O). Thus, the photolysis of nitrophenols decreases the amount of ozone lost by reaction with nitrophenoxy radicals. The impact of all the additions and modifications to the MCM on the predicted O_3 levels is shown in Figures A3, A4 of the Appendix A. Uncertainties on the reactions mentioned in this paragraph are discussed in Section 4.

Our results for ozone differ both in magnitude and sign compared to the global study by Yan et al. (2019). However, the latter used the SAPRC-11 oxidation mechanism (Carter and Heo, 2013) which does not account for the reaction of phenoxy radicals with ozone (R3) and phenylperoxy radicals with NO_2 (R2).

3.3 Inorganic nitrogen

The simulated annual mean NO_x concentrations at the surface are significantly lower in *AROM* than in *NOAROM* (Figs. 10 and 11). One reason is the formation of aromatic species containing nitrogen (e.g., nitrophenols) in *AROM*, thereby transferring part of the NO_x burden to the nitrogenated species. The largest decreases (both absolute and relative) are found in regions with high NO_x concentrations. Since the ozone chemistry is not NO_x-limited in these regions, the impact on ozone is small. This holds for the free troposphere for which zonal average decreases in NO_x can be larger than 20 % (not shown), which in turn significantly influence OH (Fig. 5).

On the one hand, the reaction with aromatics is a sink for NO_3. On the other hand, NO_3 is produced in the phenylperoxy reaction with NO_2 (R2). ~~Comparing *AROM* to~~ However the latter seems to dominate and cause a significant and widespread increase in the predicted NO_3 levels. Relative to *NOAROM*, in *AROM* the global average of the nighttime species NO_3 increases by more than 7 % (~~Tab.~~Table 3). In contrast to the global mean tendency, NO_3 modest decreases in several regions in Africa, South America, and India (Fig. 12). These decreases correlate well with emissions from biomass burning. Differences for NO_3 between the *AROM* and *onlyMCM* simulations are shown in Figures A5 of the Appendix A.

Although the net change of global HONO is small (about 3 % less in *AROM* than in *NOAROM*, see Figure 13 and ~~Tab.~~Table 3), the regional differences can be large (~~Tab.~~Table 5). A decrease of HONO is seen mainly in polluted areas (EAS, EUR, EUS) in the winter. In contrast, HONO increases in the regions with emissions from biomass burning (AMA, CAF). Here, HONO is formed by the photolysis of nitrophenols (R1). Since these reactions are not included in the MCM, we do not see any HONO increase in the *ONLYMCM* simulation (Fig. 14).

On a global average level, HNO_3 is not affected much by aromatics. However, an increase can be seen in the regions where ozone increases (EAS) or where biomass burning decreases NO_3 and N_2O_5 (CAF), see Figure 15 and ~~Tab.~~Table 5. An average zonal mean change of up to 5% throughout the UT/LS is linked to the enhanced NO_3 production by R2.

3.4 Selected oxygenated compounds

Globally, HCHO is not affected much by aromatics. There are, however, regional differences that are moderate because of the concurrent enhancement of the HCHO sink by reaction with OH. We find maximum absolute depletions in the AMA region, where concentrations are typically high (Fig. 16). Increased values of HCHO are mainly seen in EAS and EUR (~~Tab.~~Table 5).

α-dicarbonyls like glyoxal and methyl glyoxal are primarily produced from the bicycloalkyl-radical pathway leading in the case of benzene to BZBIPERO2 (MCM) (Volkamer et al., 2001). A minor secondary formation pathway from conjugated unsaturated dicarbonyls, e.g., MALDIAL (MCM), is also known and taken into account (Bloss et al., 2005b). As expected, the model predicts a very large increase of glyoxal in almost all continental areas (Figs. 17 and 18). The global burden is 36 % higher than in the *NOAROM* model simulation. The largest regional increases are in the EAS and EUR regions (~~Tab.~~Table 5). An exception to the global trend is the AMA region, where OH is too low to produce either glyoxal or methyl glyoxal. Annual mean increases exceed 50 % over the continents close to the surface. In the lower troposphere, zonal mean increases are in the 10-20 % range. These changes are of significance for the model SOA budget since these two dicarbonyls are estimated to produce a large fraction of SOA by cloud processing ~~(Lin et al., 2012).~~ yielding low-volatile oligomers (Lin et al., 2012). However, a model assessment of SOA formation from α-dicarbonyls is beyond the scope of this study. The reason is that, although the simulations were performed with a VBS-based approach to model condensation of organic vapours, the EMAC model version used in this study has no representation of oligomer formation from (methyl)glyoxal. This has been recently implemented explicitly for cloud droplets (Rosanka et al., 2020) and its effect is planned to be assessed in a subsequent study together with the contribution of reactive uptake of epoxides from isoprene and aromatics.

Comparing *AROM* to *ONLYMCM*, benzaldehyde decreases by more than 50 % when the photolysis rate constant (j-value) from the MCM (based on methacrolein) is replaced by our value (based on the UV/VIS spectrum of benzaldehyde). The more realistic photolysis rate enhances the production of radicals like HO_2.

Since additional reactive carbon compounds have been introduced in the model, the oxidation of aromatics produces more CO, which has a lifetime of about 1-3 months (Lelieveld et al., 2016). CO can travel long distances from its source, although its lifetime is not long enough to allow it to cross hemispheres (Daniel and Solomon, 1998). CO concentrations generally increase on the global scale, indicating a small addition to the carbon budget. When comparing *AROM* to *NOAROM*, we find an increase of about 6 % in the atmospheric burden of CO. Interestingly, maximum zonal average increases of 10-20 % ~~(not shown)~~ are found for the NH upper troposphere/lower stratosphere (UTLS) region ~~.~~ (Fig. 19).

4 Model uncertainties

The model calculations presented in this work are associated with some uncertainties related to the oxidation kinetic model~~and emissions .~~, emissions and model resolution.

Gas-phase oxidation of aromatics is complex and the kinetic mechanism used in this study reflects the state of knowledge, advancements and limitations in the mechanism have recently been discussed (Vereecken, 2019). Recent progress has focused in particular on the source strength of aerosol precursors and not on the overall radical production which also affects ozone. Nevertheless, our kinetic model makes use of only one rate constant for the reaction R3 of phenoxy radicals with ozone (Tao and Li, 1999). It also assigns this rate constant to the substituted phenoxy radicals other than C_6H_5O. Unfortunately, there is only one study of the rate constant of R3 at 298 K. Although the 2-σ reported uncertainty is slightly larger than 10 %, the rate constant of $2.86\times10^{-13}\ \mathrm{cm^3\ molecules^{-1}\ s^{-1}}$ has to be regarded as a lower limit. On the other hand, experimental evidence for the product of R3, being phenyl peroxy radical ($C_6H_5O_2$), has not been found although it was expected. If the products are different, then the catalytic O_3-destruction cycle illustrated in Sec. 3.2 would not be in place. However, a significant amount of ozone loss via R3 and analogous reactions is to be expected. Moreover, the ozone loss is likely underestimated because of the model not accounting for the photolysis of nitrophenols ~~reforming phenoxy~~ forming nitrosophenoxy radicals. Different from the HONO-formation channel, which destroys the aromatic ring, channels yielding substituted phenoxy radicals may dominate (Cheng et al., 2009; Vereecken et al., 2016) and thus enhance ozone loss. Another source of uncertainty is the direct formation of epoxide upon addition of OH and subsequently by O_2 as implemented in the MCM ranging from 11.8 %, for benzene, to 24 %, for trimethylbenzene (Bloss et al., 2005b,a). There in fact consistent theoretical evidence that the epoxide formation pathway passes through a second O_2-addition. This implies that the epoxide yield likely depends on the abundance of $\mathrm{NO}, \mathrm{HO_2} \mathrm{and} \mathrm{RO_2}$ (Vereecken, 2019, and references therein). This uncertainty limit the reliability of the predicted SOA formation from reactive uptake of epoxides by aerosols (Paulot et al., 2009).

Cloud chemistry of organic compounds is known to suppress gas-phase HO_x-production and directly consume ozone (Lelieveld and Crutzen, 1990). The overall effect on ozone depends on the local chemical regime. In our study water-soluble products are set to only undergo wet deposition (dissolution and removal by precipitation). Their aqueous-phase chemistry might however have a non-negligible effect on ozone and other oxidants. For instance, phenol is known to react very quickly with OH in the aqueous-phase (Field et al., 1982). Moreover, phenoxide anions from phenols react quickly with ozone (Hoigné and Bader, 1983). In particular, nitrophenols might be efficient ozone scavengers as they are stronger acids than unsubstituted phenols. A global assessment of cloud chemistry involving aromatics oxidation products is possible with the modelling system used here (Tost et al., 2006, 2010). However, considering the complexity of aqueous-phase oxidation of organic compounds, such an assessment is outside the scope of this study and deserves a dedicated model study.

In our study, biomass burning emissions of aromatics are potentially underestimated. In fact, based on the recent update by Andreae (2019), we estimate that emissions might be up to 5 $\mathrm{Tg/a}$ (65%) higher than what is implemented in our model. Moreover, emissions from peat fires in 2010 (the simulated year) were up to a factor 15 lower than in the subsequent years (van der Werf et al., 2017). In general, the inter-annual variability of biomass burning is large and difficult to capture in a study such as the present one. However, it appears that the two major contributions to this variability are the peat fires in Indonesia and boreal forest fires, which are strongly favoured by El Nino and heat waves, respectively. An early estimate of anthropogenic emissions of aromatics gave 16 TgC/a, (Fu et al., 2008). Two relatively recent datasets yield about 50% higher emissions being 23 TgC/a for RCP (Cabrera-Perez et al., 2016) and 22 TgC/a for EDGAR 4.3.2 (Huang et al., 2017). The latter is used in this study and lacks the biofuel burning emissions of phenol, benzaldehyde and styrene. Inter-annual variability of anthropogenic emissions of aromatics is is not well known but the decadal trends are known to be negative since the 1980s (Lamarque et al., 2010). Aromatics emissions from terrestrial vegetation have been long neglected or considered very low. However, Misztal et al. (2015) suggested that aromatics emissions from biogenic sources may rival those from anthropogenic ones. In this study we used the same emission algorithm used in Misztal et al. (2015) but get much lower emissions for toluene (about 0.3 vs. 1.5 TgC/a). However, Misztal et al. (2015) suggest that emissions of aromatics and benzenoid compounds may be in the 1.4-15 TgC/a range. The major contributors are toluene and some benzenoids (oxygenated aromatics). The latter are mainly emitted during blossoming and stress-induced reactions by plants. The variability of their emissions is not very well quantified. For instance, the MEGAN model calculates their emission strengths based of the ones for carbon monoxide (Tarr et al., 1995).

The spatial resolution of atmospheric models has a significant influence on the predicted levels of oxidants and nitrogen oxides. Generally in polluted regions the coarser the resolution the larger the ozone production per molecule of $\mathrm{NO_x}$ will be (Sillman et al., 1990). This is due to the artificial dilution of strong NOx emissions which, in reality, is efficiently converted to $\mathrm{NO_y}$ by reacting with $\mathrm{HO_x}$. For instance, reducing the spatial resolution over the polluted North America, Europe and East Asia with a two-way nested regional model led to a 9.5 % reduction in the global tropospheric ozone burden (Yan et al., 2016). We have shown that at our model resolution of $1.875° \times 1.875°$ aromatics are estimated to induce important increases in $\mathrm{HO_x}$ (Fig. 3) and decreases in $\mathrm{NO_x}$ (Fig. 10 and 11) over continental polluted regions. Therefore, at much higher spatial resolutions we expect that the enhancement of surface ozone by aromatics in those regions (Fig. 6) to be greatly reduced if not reverted. Based on the results by Yan et al. (2016) we expect this effect to translate in a significant enhancement of the tropospheric ozone reduction reported in this study (Sect. 3.2). A quantification of the model resolution effect on chemical regimes is at the moment computationally prohibitive with our very large chemical scheme running in the global EMAC model.

Finally, atmospheric levels of benzene and toluene simulated by our model were shown to underestimate many observations by at least 20% (Cabrera-Perez et al., 2016). It is worth noting that in Cabrera-Perez et al. (2016) the total emissions of aromatics were even slightly higher (2.6 $\mathrm{TgC/yr}$) than in the *AROM* simulation. This underestimate could be explained by an overestimate of the chemical sink in the troposphere by reaction with hydroxyl radical. However, the annual global mean concentration of hydroxyl radicals is potentially 10% too high (Lelieveld et al., 2016), which cannot account for model concentration biases that are larger than 20%. Therefore, we surmise that the impact of aromatics on the trace gas composition may be larger than estimated in this study.

5 Summary

This study investigates the effects of several monocyclic aromatics on the tropospheric gas-phase composition by means of the chemistry-climate model EMAC. When aromatics are introduced into our model calculations, large changes are seen for glyoxal and methyl glyoxal. For other species, our results show a relatively small importance of aromatics on the global scale. This is consistent with recent results by Yan et al. (2019) who used a simpler chemistry mechanism in the GEOS-Chem model. However, different from that study, we found a negative impact on global ozone. Our results also indicate that by including aromatics chemistry, free tropospheric OH is reduced, especially in the northern hemisphere. On a regional scale, the concentrations of several species change significantly, with relatively largest impacts in East Asia where emissions are higher. Regions with high $\mathrm{NO_x}$ concentrations show increases of OH and $\mathrm{O_3}$. However, since these increases are counteracted by decreases downwind, i.e., in remote areas where $\mathrm{NO_x}$ concentrations are much lower, the net effects on large scales are small. Of the nitrogen compounds, mainly $\mathrm{NO_3}$ and HONO are affected by the aromatics chemistry.

We conclude that, although the impact of aromatics is relatively minor on the global scale, it is important on regional scales, notably in the anthropogenic source regions, and especially in those where $\mathrm{NO_x}$ emissions are strongest. Given the uncertainties in the oxidation mechanisms and emissions, the results of our model calculations may underestimate the impact of aromatics on the tropospheric gas-phase composition.

Code availability. The Modular Earth Submodel System (MESSy) is continuously further developed and applied by a consortium of institutions. The usage of MESSy and access to the source code is licensed to all affiliates of institutions which are members of the MESSy Consortium. Institutions can be a member of the MESSy Consortium by signing the MESSy Memorandum of Understanding. More information can be found on the MESSy Consortium web-page (http://www.messy-interface.org).

Author contributions. DT, RS, AP and DC wrote the manuscript. AP and DC performed the model simulations. DT and RS developed and analyzed the chemical mechanism. SB visualized the model results. SG performed extended budgeting of species' chemical turnover. All co-authors contributed to the analysis of results and the writing of the paper.

Competing interests. The authors have no competing interests

Acknowledgements. The authors want to acknowledge the use of the Ferret program for analysis and graphics in this paper. Ferret is a product of NOAA's Pacific Marine Environmental Laboratory (information is available at http://www.ferret.noaa.gov). The work described in this paper has received funding from the Initiative and Networking Fund of the Helmholtz Association through the project "Advanced Earth System Modelling Capacity (ESM)" (information is available at https://www.esm-project.net/).

Table 1. Global annual emission rates of aromatic compounds included in the model simulations and their relative contributions.

Species	total (TgC/a)	anthro-pogenic (EDGAR)	biomass burning (BIOBURN)	biogenic (MEGAN)
Benzene	4.417	70 %	30 %	
Toluene	5.888	82 %	13 %	5 %
Xylenes	5.664	96 %	4 %	
Ethylbenzene	1.961	74 %	26 %	
Benzaldehyde	1.382	92 %	6 %	2 %
Phenol	2.559	43 %	57 %	
Styrene	1.596	91 %	9 %	
Trimethylbenzenes	0.906	94 %	6 %	
Higher aromatics	4.980	48 %	52 %	

Table 2. Sensitivity studies.

Simulation	Description
AROM	Aromatics are fully included
NOAROM (reference)	No aromatics (emissions switched off)
ONLYMCM	Only MCM reactions

Table 3. Globally averaged area-weighted mixing ratios at the surface (annual averages for 2010). "ABSDIFF" denotes the absolute difference, (e.g., AROM-NOAROM), and "RELDIFF" the relative difference, (e.g., AROM/NOAROM-1).

				AROM vs *ONLYMCM*		*AROM* vs *NOAROM*	
	NOAROM	*ONLYMCM*	*AROM*	ABSDIFF	RELDIFF	ABSDIFF	RELDIFF
	mol/mol	mol/mol	mol/mol	mol/mol	%	mol/mol	%
OH	4.630×10^{-14}	4.472×10^{-14}	4.487×10^{-14}	1.557×10^{-16}	0.3482	-1.425×10^{-15}	-3.078
O_3	3.269×10^{-8}	3.220×10^{-8}	3.190×10^{-8}	-2.964×10^{-10}	-0.9204	-7.888×10^{-10}	-2.413
NO	3.029×10^{-11}	2.793×10^{-11}	2.609×10^{-11}	-1.843×10^{-12}	-6.599	-4.203×10^{-12}	-13.87
NO_2	3.389×10^{-10}	3.314×10^{-10}	3.191×10^{-10}	-1.228×10^{-11}	-3.706	-1.977×10^{-11}	-5.834
NO_3	1.004×10^{-12}	9.462×10^{-13}	1.080×10^{-12}	1.339×10^{-13}	14.15	7.599×10^{-14}	7.568
HONO	7.393×10^{-12}	7.260×10^{-12}	7.315×10^{-12}	5.538×10^{-14}	0.7628	-7.754×10^{-14}	-1.049
HNO_3	1.420×10^{-10}	1.393×10^{-10}	1.426×10^{-10}	3.352×10^{-12}	2.407	6.607×10^{-13}	0.4653
HCHO	5.993×10^{-10}	5.992×10^{-10}	6.002×10^{-10}	9.484×10^{-13}	0.1583	8.414×10^{-13}	0.1404
glyoxal	1.040×10^{-11}	1.444×10^{-11}	1.505×10^{-11}	6.117×10^{-13}	4.237	4.646×10^{-12}	44.67
methyl glyoxal	3.847×10^{-11}	4.005×10^{-11}	4.015×10^{-11}	1.051×10^{-13}	0.2625	1.682×10^{-12}	4.372
benzaldehyde		6.798×10^{-12}	4.479×10^{-12}	-2.319×10^{-12}	-34.11	4.479×10^{-12}	
CO	97.6×10^{-9}	103.3×10^{-9}	103.3×10^{-9}	-6.5×10^{-11}	-0.06278	5.7×10^{-9}	5.847

Table 4. Simulated tropospheric integrals of OH, O_3 and NO_x, and the lifetime τ of CH_4. Tropospheric burdens were reckoned using six different tropopause definitions (provided by the TROPOP submodel, see Jöckel et al. (2010) for details): 1,2 surfaces of O_3 mixing ratio of 125 and 150 nmol/mol, respectively, 3) WMO definition (WMO (1957)), 4) dynamic PV-based (3.5 PVU potential vorticity surface, sought within 50–800 hPa), 5) climatological (invariable zonal profile, i.e. 300-215•(cos(latitude))^2 hPa) and 6) the combined definition (WMO tropopause within 30°N–30°S, otherwise dynamic PV-based tropopause). The latter definition is used by default in EMAC and in this work. Estimated changes to tropospheric O_3 burden are identical within 0.05 % between the available definitions.

	n(OH)		$m(O_3)$		$n(NO_x)$		$\tau(CH_4)$	
Simulation	NH	SH	NH	SH	NH	SH	NH	SH
NOAROM	6799 kmol	5765 kmol	207 Tg	173 Tg	7.90 Gmol	4.02 Gmol	7.36 yrs	9.61 yrs
ONLYMCM vs *NOAROM*	−9.9 %	−7.3 %	−2.5 %	−2.1 %	−3.7 %	−1.0 %	+7.1 %	+4.7 %
AROM vs *NOAROM*	−9 %	−6.3 %	−3.5 %	−2.3 %	−10.8 %	−4.5 %	+6.8 %	+4.5 %

Table 5. Regionally averaged mixing ratios of selected species (annual averages for 2010).

	NOAROM mol/mol	*AROM* mol/mol	ABSDIFF mol/mol	RELDIFF %
		OH		
AMA	2.861×10^{-14}	2.785×10^{-14}	-7.689×10^{-16}	-2.687
CAF	6.447×10^{-14}	6.086×10^{-14}	-3.616×10^{-15}	-5.608
EAS	4.712×10^{-14}	5.527×10^{-14}	8.147×10^{-15}	17.29
EUR	3.591×10^{-14}	3.852×10^{-14}	2.615×10^{-15}	7.283
EUS	5.629×10^{-14}	5.784×10^{-14}	1.553×10^{-15}	2.759
		O_3		
AMA	2.979×10^{-8}	2.909×10^{-8}	-6.973×10^{-10}	-2.341
CAF	3.856×10^{-8}	3.712×10^{-8}	-1.440×10^{-9}	-3.733
EAS	3.124×10^{-8}	3.505×10^{-8}	3.807×10^{-9}	12.19
EUR	3.045×10^{-8}	3.033×10^{-8}	-1.250×10^{-10}	-0.4105
EUS	3.930×10^{-8}	3.904×10^{-8}	-2.604×10^{-10}	-0.6626
		NO_3		
AMA	3.570×10^{-13}	3.483×10^{-13}	-8.678×10^{-15}	-2.431
CAF	2.105×10^{-12}	2.321×10^{-12}	2.163×10^{-13}	10.27
EAS	1.833×10^{-12}	1.949×10^{-12}	1.163×10^{-13}	6.346
EUR	1.280×10^{-12}	1.256×10^{-12}	-2.448×10^{-14}	-1.913
EUS	2.536×10^{-12}	2.488×10^{-12}	-4.802×10^{-14}	-1.894
		HONO		
AMA	5.335×10^{-11}	5.349×10^{-11}	1.370×10^{-13}	0.2567
CAF	8.110×10^{-11}	8.227×10^{-11}	1.174×10^{-12}	1.447
EAS	1.152×10^{-10}	1.038×10^{-10}	-1.146×10^{-11}	-9.945
EUR	5.689×10^{-11}	5.604×10^{-11}	-8.429×10^{-13}	-1.482
EUS	4.415×10^{-11}	4.230×10^{-11}	-1.854×10^{-12}	-4.199
		HNO_3		
AMA	1.515×10^{-10}	1.508×10^{-10}	-7.056×10^{-13}	-0.4657
CAF	4.957×10^{-10}	5.162×10^{-10}	2.048×10^{-11}	4.131
EAS	1.035×10^{-9}	1.169×10^{-9}	1.335×10^{-10}	12.89
EUR	3.985×10^{-10}	4.003×10^{-10}	1.855×10^{-12}	0.4656
EUS	6.706×10^{-10}	6.721×10^{-10}	1.505×10^{-12}	0.2244
		HCHO		
AMA	5.217×10^{-9}	5.189×10^{-9}	-2.874×10^{-11}	-0.5509
CAF	3.468×10^{-9}	3.478×10^{-9}	9.392×10^{-12}	0.2708
EAS	1.322×10^{-9}	1.557×10^{-9}	2.348×10^{-10}	17.76
EUR	7.356×10^{-10}	7.708×10^{-10}	3.517×10^{-11}	4.781
EUS	1.911×10^{-9}	1.942×10^{-9}	3.096×10^{-11}	1.620

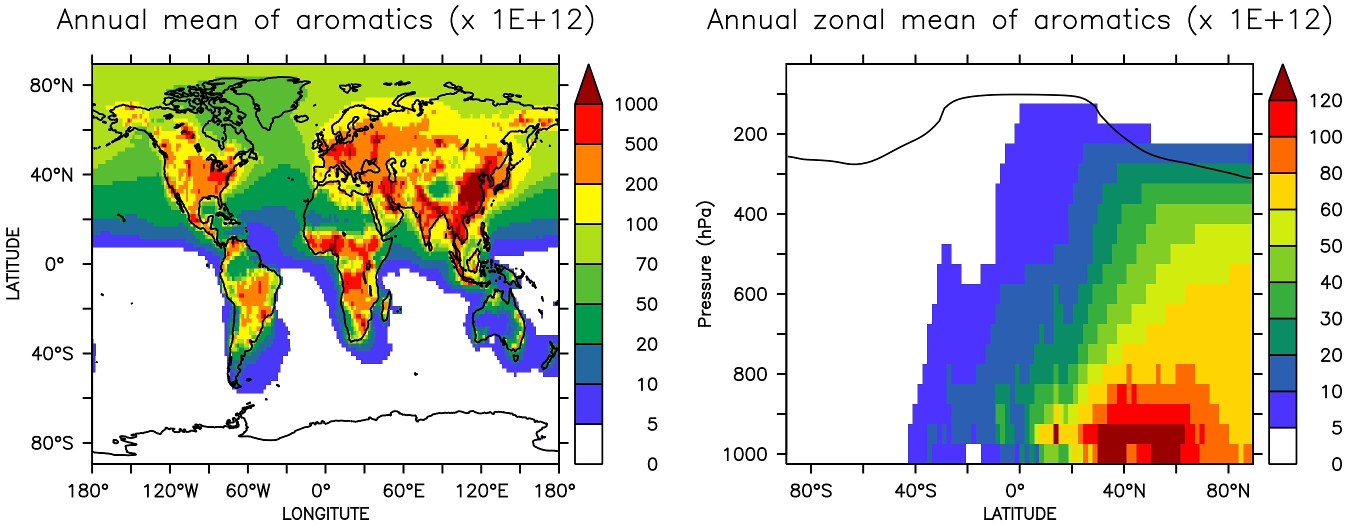

Figure 1. Annual mean mixing ratios of the sum of aromatics at the surface (left) and the zonal mean (right) in the *AROM* simulation. The solid line between 100 and 300 hPa depicts the mean tropopause level.

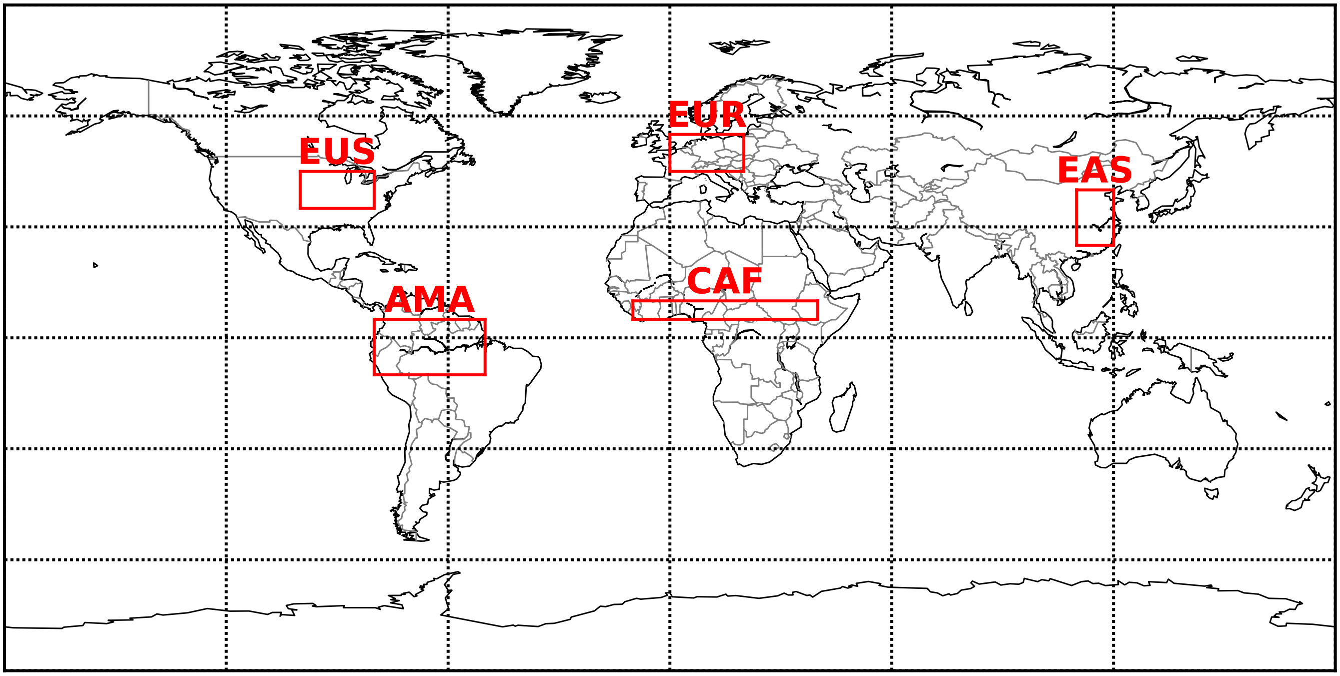

Figure 2. Selected regions: AMA = Amazon area, CAF = central Africa, EAS = eastern Asia, EUR = Europe, EUS = eastern US.

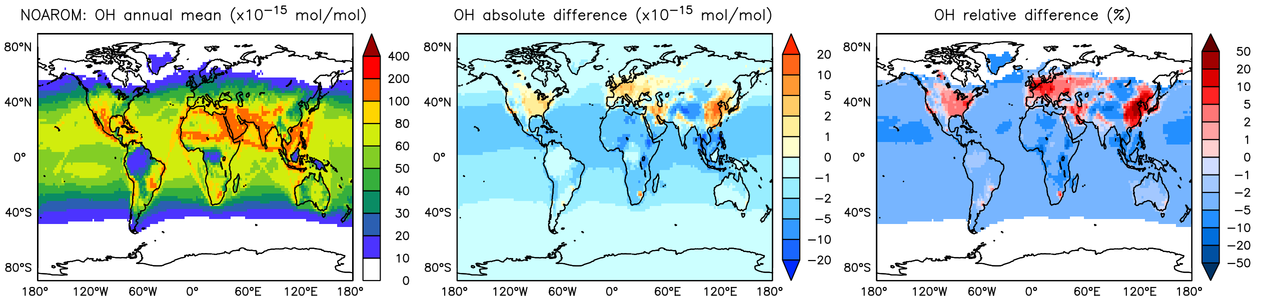
NOAROM: OH annual mean (x10^{-15} mol/mol)
OH absolute difference (x10^{-15} mol/mol)
OH relative difference (%)
80°N
40°N
0°
40°S
80°S
180°
120°W
60°W
0°
60°E
120°E
180°
400
200
100
80
60
50
40
30
20
10
0
20
10
5
2
1
0
−1
−2
−5
−10
−20
50
20
10
5
2
1
0
−1
−2
−5
−10
−20
−50

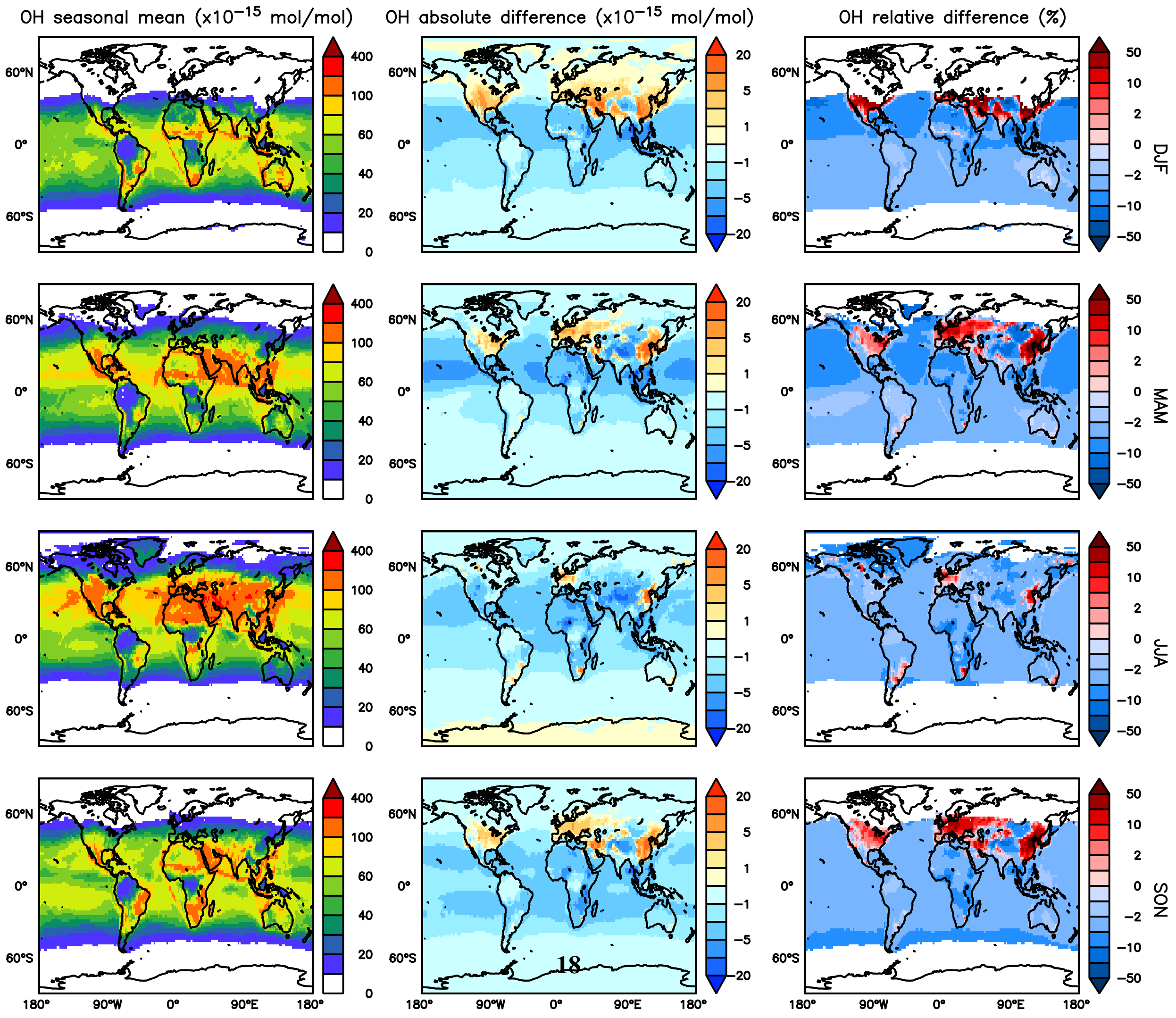
OH seasonal mean (x10^{-15} mol/mol)
OH absolute difference (x10^{-15} mol/mol)
OH relative difference (%)
60°N
0°
60°S
180°
90°W
0°
90°E
180°
400
100
60
40
20
0
20
5
1
−1
−5
−20
50
10
2
0
−2
−10
−50
DJF
MAM
JJA
SON

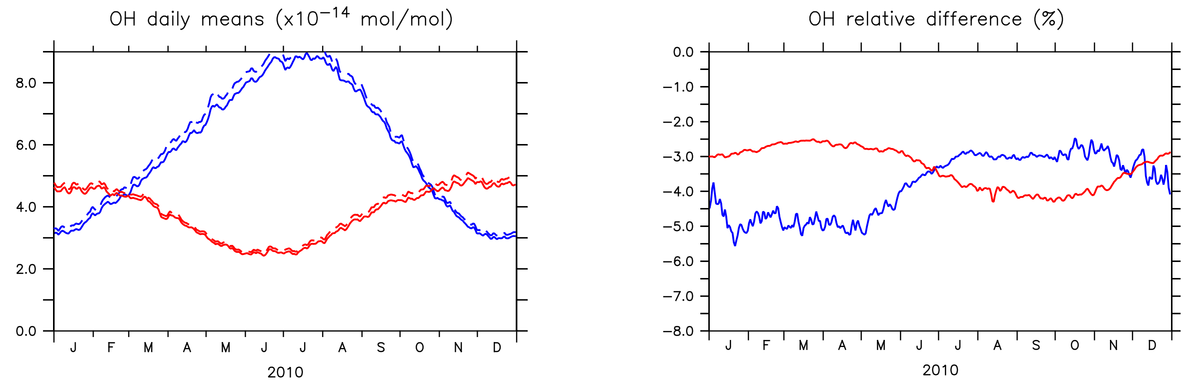

Figure 4. Left: Seasonal ~~cycle~~ cycles of OH daily (24 h) mixing ratio means (in 10^{-14} mol/mol) in the planetary boundary layer (PBL) for AROM (solid line) and ~~relative~~ NOAROM (dashed line). Right: Relative difference (expressed in %) between ~~*AROM* (solid)~~ AROM and ~~*NOAROM* (dashed)~~NOAROM. In blue, values for the NH; in red, values for the SH. The PBL diagnosis is described in Pozzer et al. (2009). The PBL is calculated in the model based on the work of Holtslag et al. (1990). An interactive calculation is performed following the approach of Troen and Mahrt (1986), using the Richardson number, the horizontal velocity components, the buoyancy parameters and the virtual temperature (Holtslag and Boville, 1993).

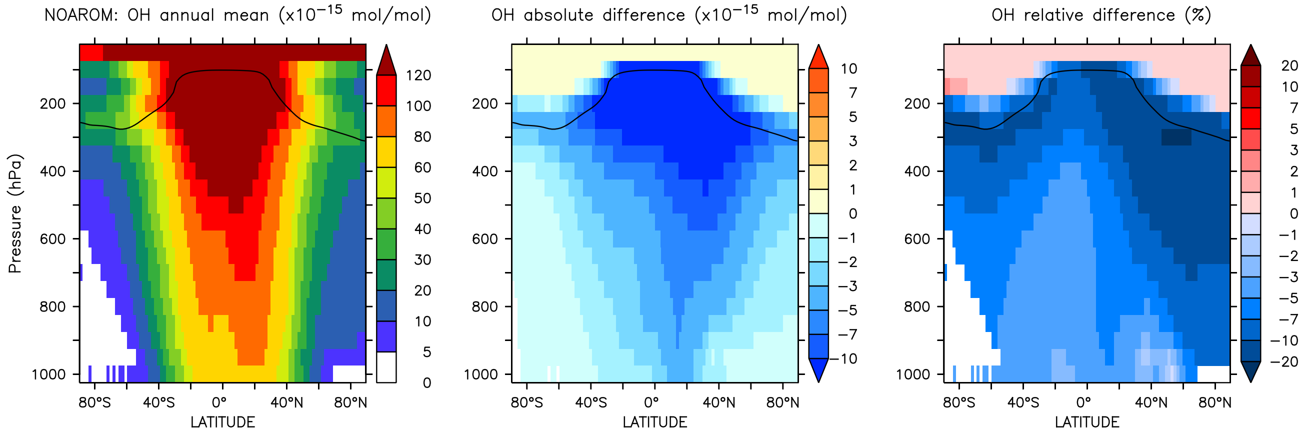

Figure 5. Annual average zonal mean OH mixing ratios. Left: Mixing ratios in the *NOAROM* simulation. Middle: Absolute difference *AROM-NOAROM*. Right: Relative difference *AROM/NOAROM*-1 in %. The solid line between 100 and 300 hPa depicts the mean tropopause level.

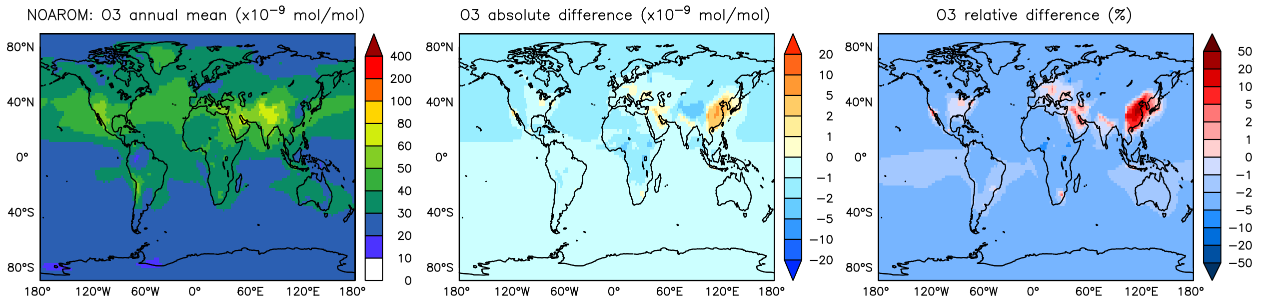

Figure 6. Annual average O_3 mixing ratios at the surface. Left: Mixing ratios in the *NOAROM* simulation. Middle: Absolute difference *AROM-NOAROM*. Right: Relative difference *AROM/NOAROM*-1 in %.

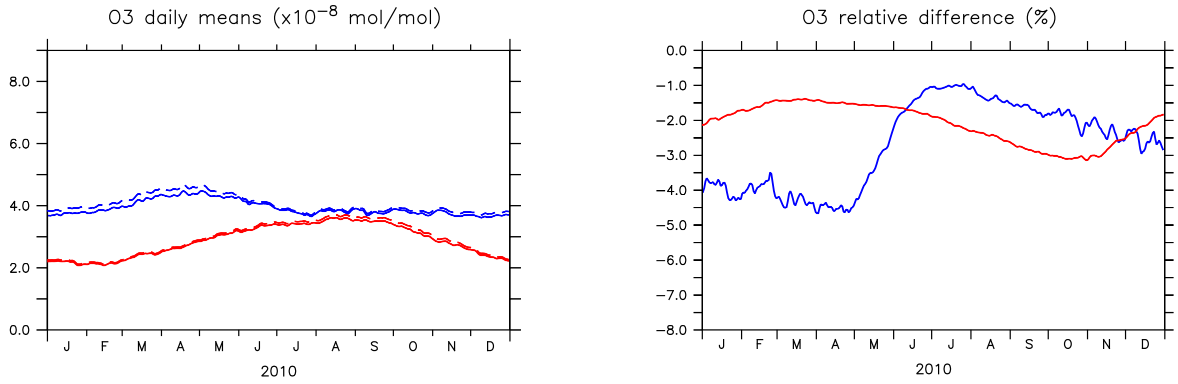

Figure 7. Same as in Fig. 4 for ozone (the unit in the left plot is 10^{-8} mol/mol.**((TO BE UPDATED))**

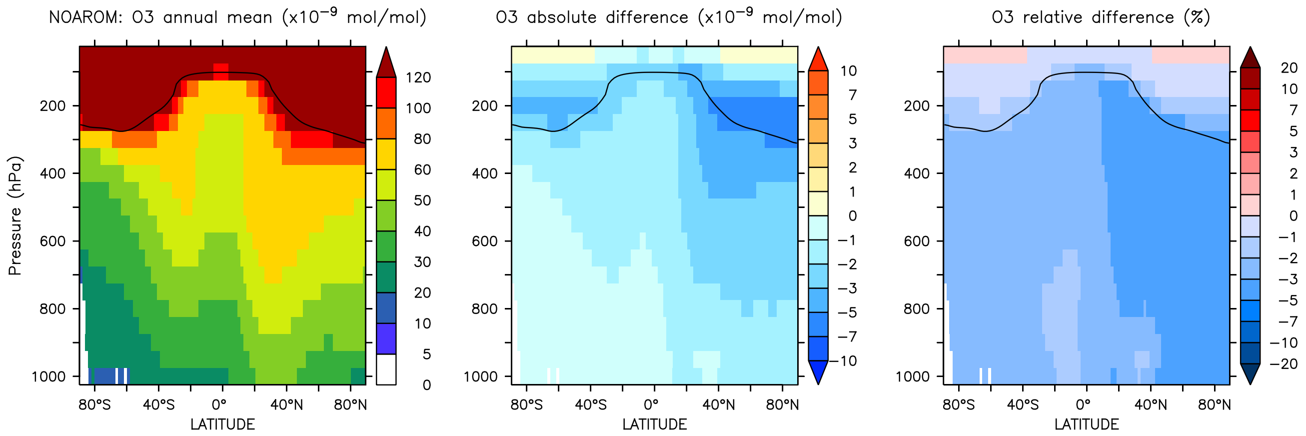

Figure 8. Annual average zonal mean O_3 mixing ratios. Left: Mixing ratios in the *NOAROM* simulation. Middle: Absolute difference *AROM-NOAROM*. Right: Relative difference *AROM/NOAROM*-1 in %. The solid line between 100 and 300 hPa depicts the mean tropopause level.

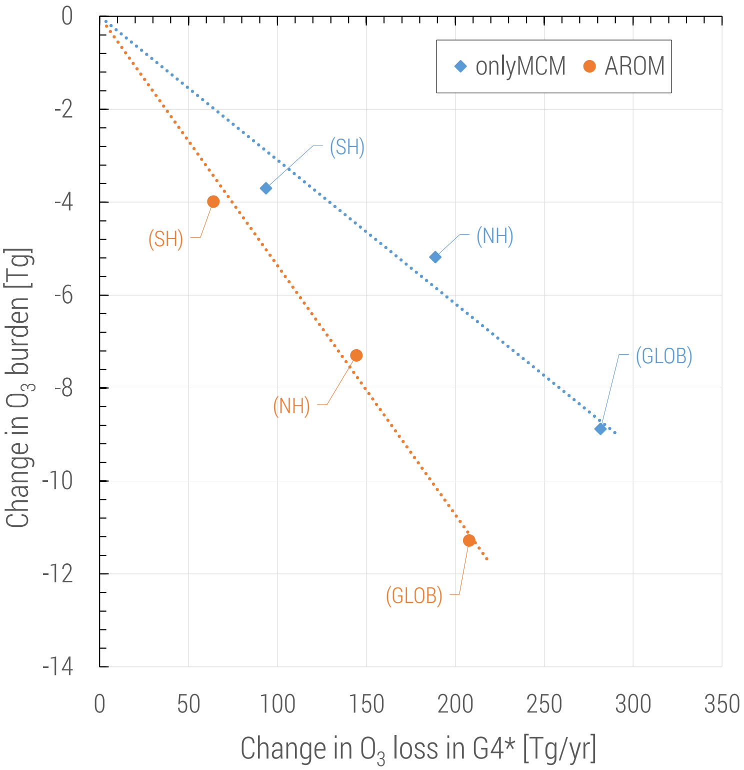

Figure 9. Change in tropospheric ozone burden versus change in ozone loss for all reactions in the VOC chemistry (G4 category of the MECCA mechanism[, see the Supplement of (Sander et al., 2019)]). The change in ozone loss is due to the reactions with (substituted) phenoxy radicals. Global and hemispheric results for *onlyMCM* (blue) and *AROM* (orange) simulations are shown.

~~Same as in Fig. 4 for ozone.~~

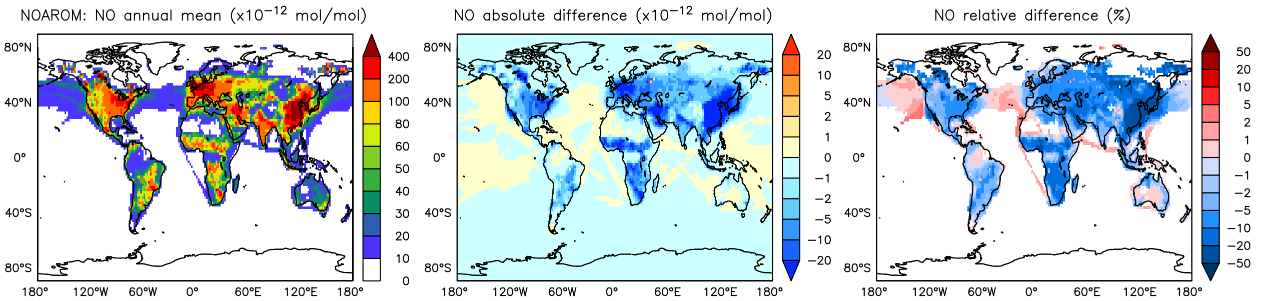

Figure 10. Annual average NO mixing ratios at the surface. Left: Mixing ratios in the *NOAROM* simulation. Middle: Absolute difference *AROM-NOAROM*. Right: Relative difference *AROM/NOAROM*-1 in % (shown only where NO is above 10 pmol/mol).

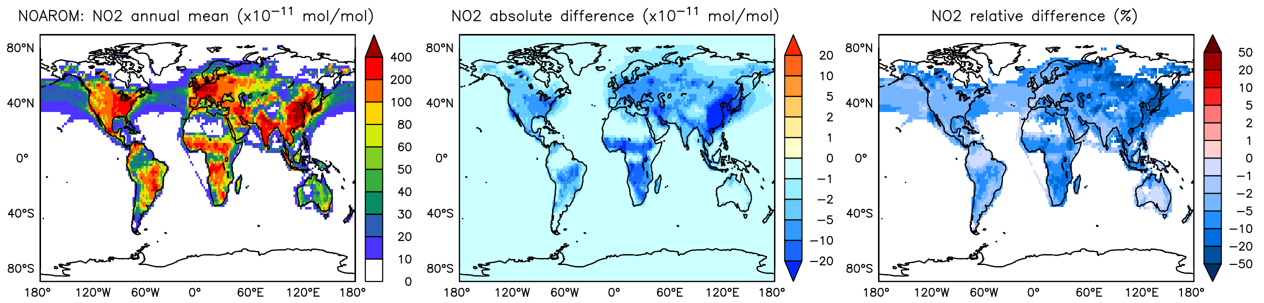

Figure 11. Annual average NO_2 mixing ratios at the surface. Left: Mixing ratios in the *NOAROM* simulation. Middle: Absolute difference *AROM*-*NOAROM*. Right: Relative difference *AROM*/*NOAROM*-1 in % (shown only where NO_2 is above 100 pmol/mol).

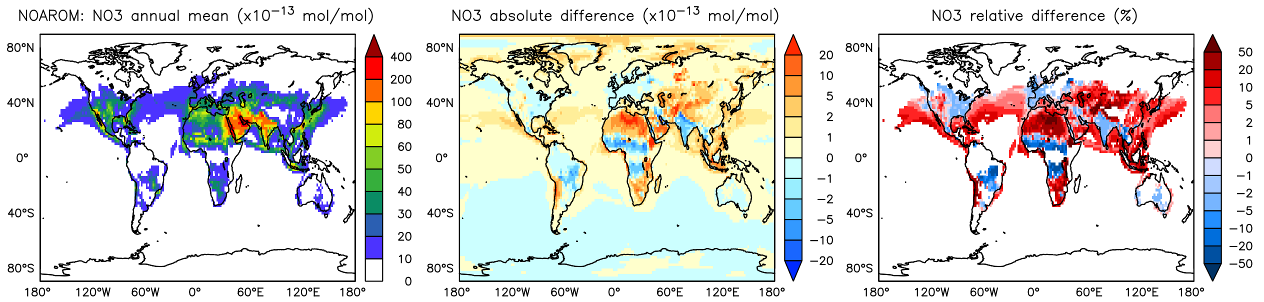

Figure 12. Annual average NO_3 mixing ratios at the surface. Left: Mixing ratios in the *NOAROM* simulation. Middle: Absolute difference *AROM*-*NOAROM*. Right: Relative difference *AROM*/*NOAROM*-1 in % (shown only where NO_3 is above 1 pmol/mol).

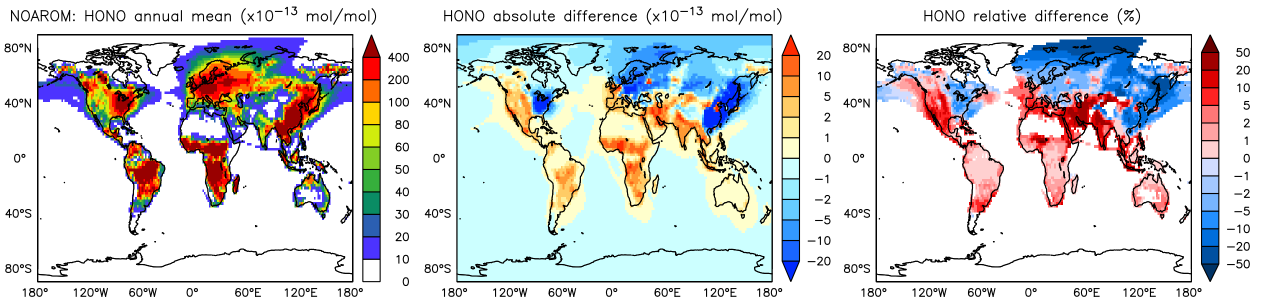

Figure 13. Annual average HONO mixing ratios at the surface. Left: Mixing ratios in the *NOAROM* simulation. Middle: Absolute difference *AROM*-*NOAROM*. Right: Relative difference *AROM*/*NOAROM*-1 in % (shown only where HONO is above 1 pmol/mol).

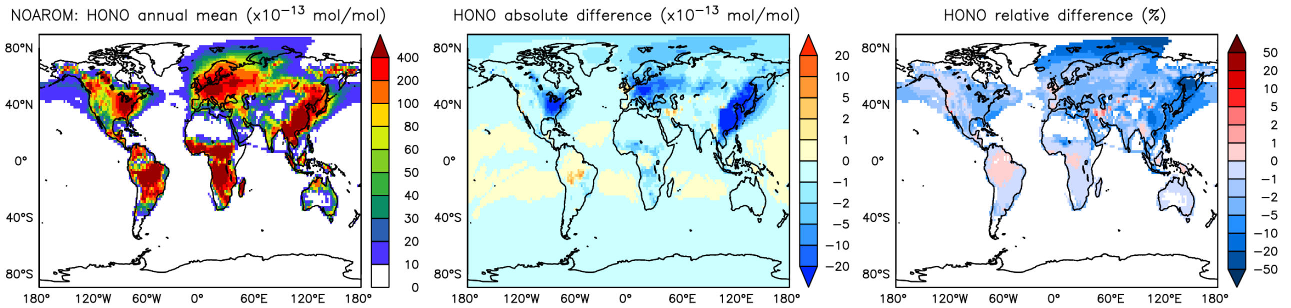

Figure 14. Annual average HONO mixing ratios at the surface. Left: Mixing ratios in the *NOAROM* simulation. Middle: Absolute difference *ONLYMCM*-*NOAROM*. Right: Relative difference *ONLYMCM*/*NOAROM*-1 in % (shown only where HONO is above 1 pmol/mol)~~.~~

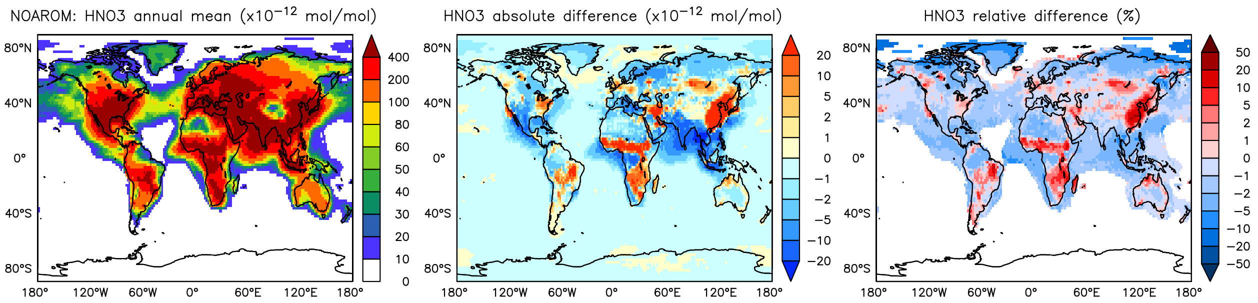

Figure 15. Annual average HNO_3 mixing ratios at the surface. Left: Mixing ratios in the *NOAROM* simulation. Middle: Absolute difference *AROM-NOAROM*. Right: Relative difference *AROM/NOAROM*-1 in % (shown only where HNO_3 is above 10 pmol/mol).

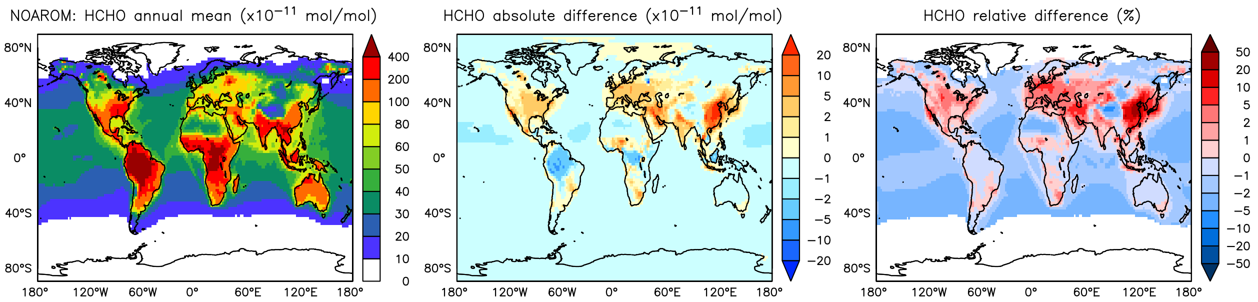

Figure 16. Annual average HCHO mixing ratios at the surface. Left: Mixing ratios in the *NOAROM* simulation. Middle: Absolute difference *AROM-NOAROM*. Right: Relative difference *AROM/NOAROM*-1 in % (shown only where HCHO is above 100 pmol/mol).

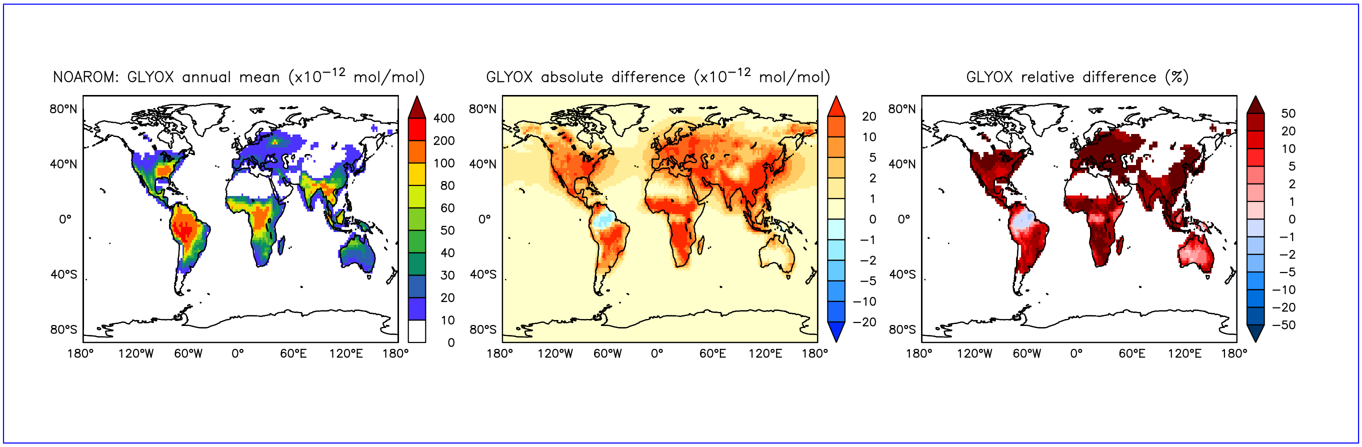

Figure 17. Annual average glyoxal mixing ratios at the surface. Left: Mixing ratios in the *NOAROM* simulation. Middle: Absolute difference *AROM-NOAROM*. Right: Relative difference *AROM/NOAROM*-1 in % (shown only where glyoxal is above 10 pmol/mol).

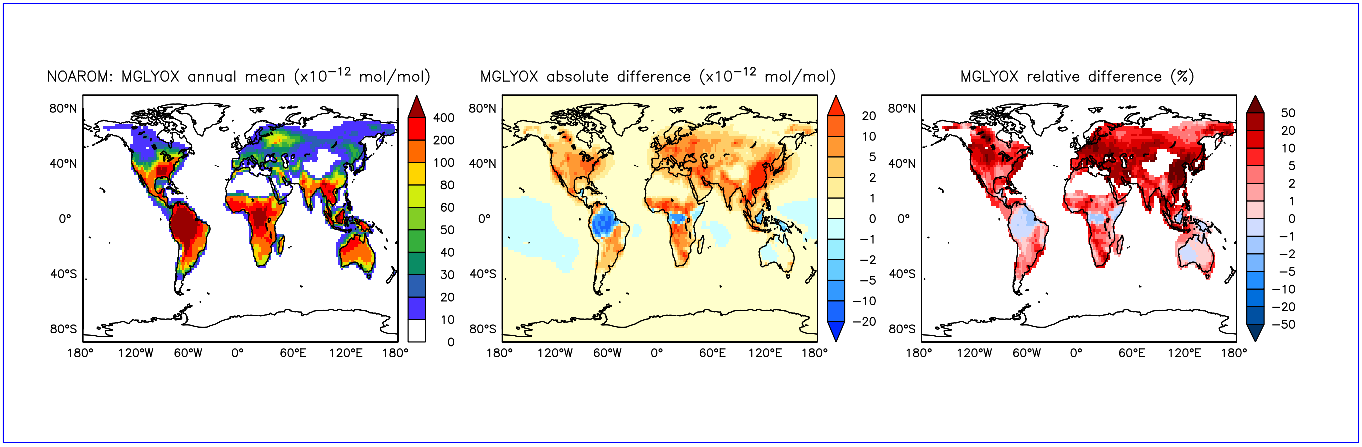

Figure 18. Annual average methyl glyoxal mixing ratios at the surface. Left: Mixing ratios in the *NOAROM* simulation. Middle: Absolute difference *AROM-NOAROM*. Right: Relative difference *AROM/NOAROM*-1 in % (shown only where methyl glyoxal is above 10 pmol/mol).

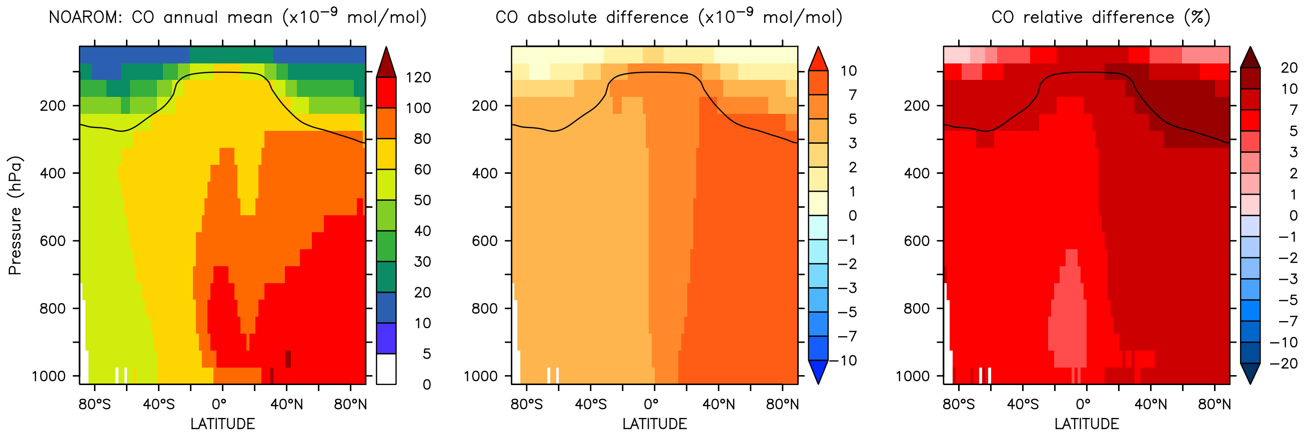

Figure 19. Annual average zonal mean CO mixing ratios. Left: Mixing ratios in the *NOAROM* simulation. Middle: Absolute difference *AROM-NOAROM*. Right: Relative difference *AROM/NOAROM*-1 in %. The solid line between 100 and 300 hPa depicts the mean tropopause level.

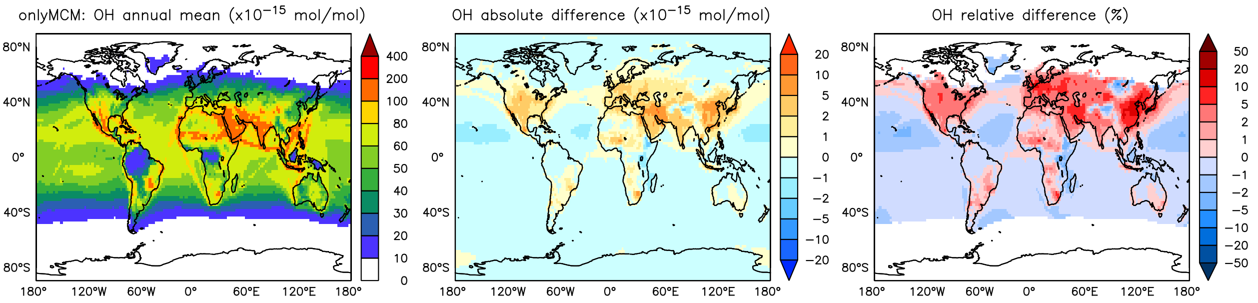

Figure A1. Annual average OH mixing ratios at the surface. Middle rows: Seasonal means. Left column: Mixing ratios in the *onlyMCM* simulation. Middle column: Absolute difference *AROM-onlyMCM*. Right column: Relative difference *AROM/onlyMCM*-1 in % (shown only where OH is above 0.01 pmol/mol).

Appendix A: *AROM vs. onlyMCM*

In this appendix the impact of the modifications to the MCM chemistry (listed in Sect. 2) on the model results are shown for the main atmospheric oxidants.

Hydroxyl radical (OH)

The differences at the surface are shown in Figure A1. Much of the increase in Figure 3 can be ascribed to the enhanced HO_x production by photolysis of benzaldehyde (Roth et al., 2010) and HONO from R1. The latter from benzene chemistry explains the significant enhancement across the UT/LS (see Fig. A2).

Ozone (O_3)

The differences at the surface are shown in Figure A3. It can be seen that lareg part of the enhancement in surface ozone mixing ratio in Figure 6 is due to enhanced HO_x production in regions that are not NO_x-limited. The zonal mean change in ozone is minimal and slightly positive at the tropical UT/LS (Fig. A4).

Nitrate radical (NO_3)

The differences at the surface are shown in Figure A5. It can be seen that the widespread enhancement of in Figure 12 is largely to be ascribed to the effect of phenylperoxy reaction with NO_2 (R2).

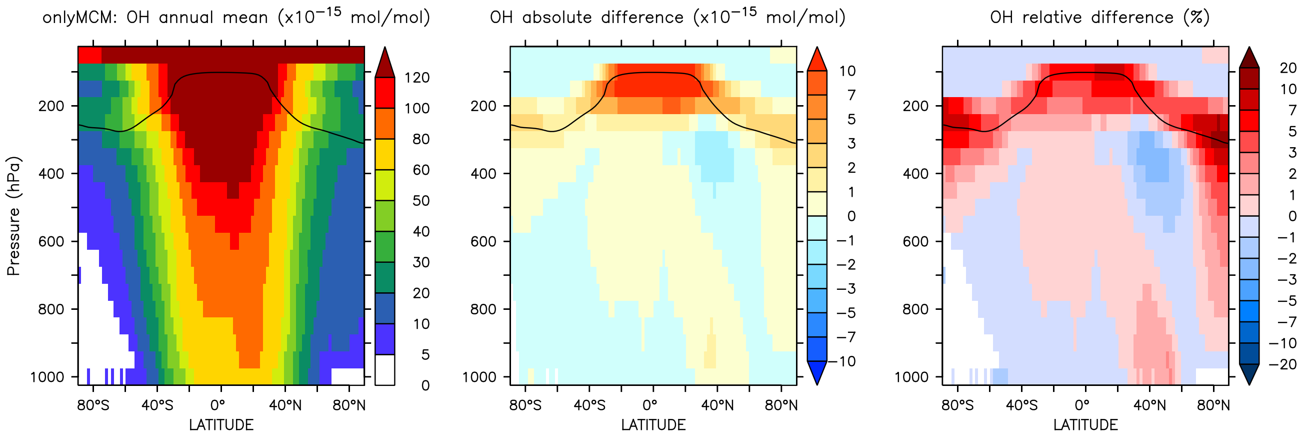

Figure A2. Annual average zonal mean OH mixing ratios. Left: Mixing ratios in the *onlyMCM* simulation. Middle: Absolute difference *AROM-onlyMCM*. Right: Relative difference *AROM*/*onlyMCM*-1 in %. The solid line between 100 and 300 hPa depicts the mean tropopause level.

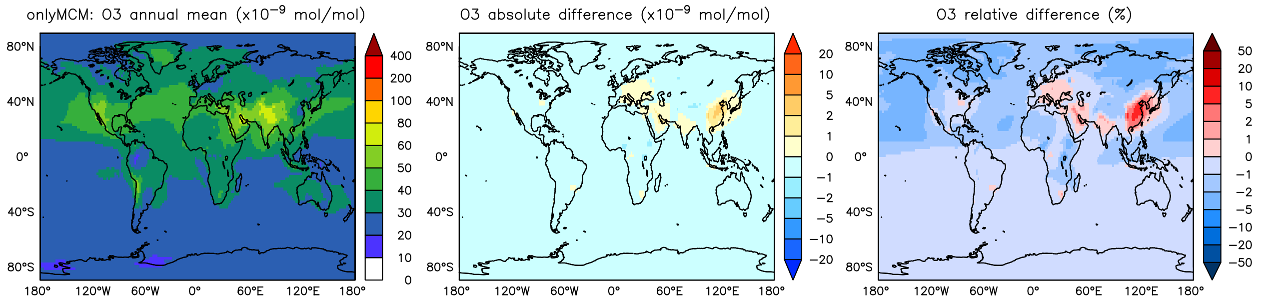

Figure A3. Annual average O_3 mixing ratios at the surface. Left: Mixing ratios in the *onlyMCM* simulation. Middle: Absolute difference *AROM-onlyMCM*. Right: Relative difference *AROM*/*onlyMCM*-1 in %.

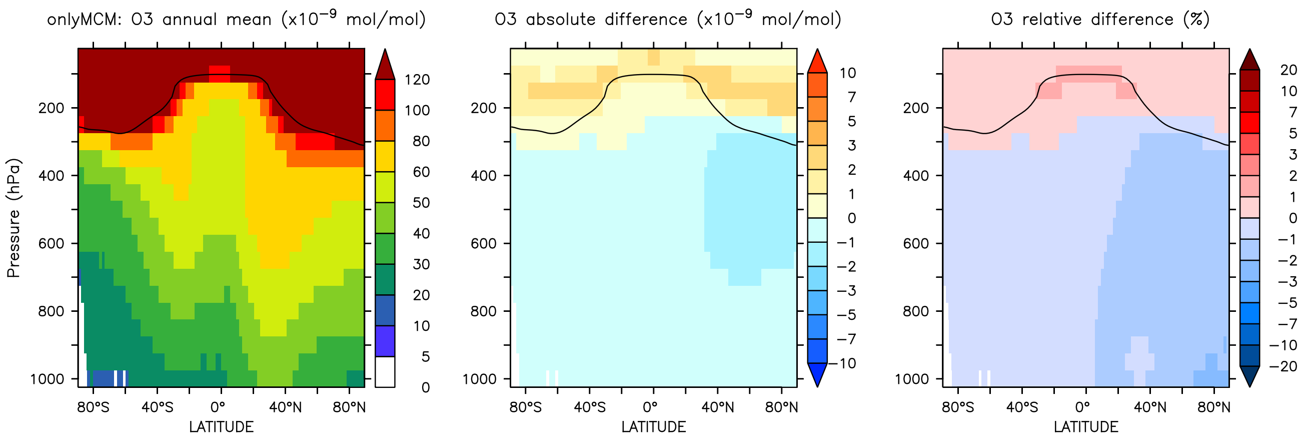

Figure A4. Annual average zonal mean O_3 mixing ratios. Left: Mixing ratios in the *onlyMCM* simulation. Middle: Absolute difference *AROM-onlyMCM*. Right: Relative difference *AROM*/*onlyMCM*-1 in %. The solid line between 100 and 300 hPa depicts the mean tropopause level.

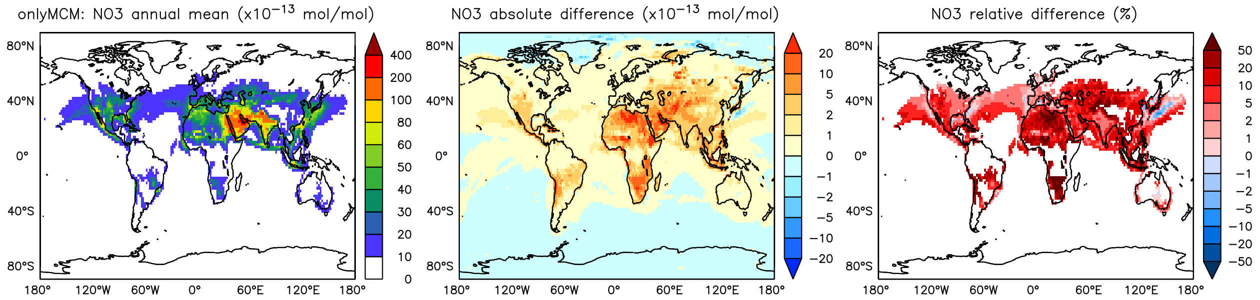

Figure A5. Annual average NO_3 mixing ratios at the surface. Left: Mixing ratios in the *onlyMCM* simulation. Middle: Absolute difference *AROM-onlyMCM*. Right: Relative difference *AROM*/*onlyMCM*-1 in % (shown only where NO_3 is above 1 pmol/mol).

References

Andreae, M. O.: Emission of trace gases and aerosols from biomass burning – an updated assessment, Atmospheric Chemistry and Physics, 19, 8523–8546, https://doi.org/10.5194/acp-19-8523-2019, https://www.atmos-chem-phys.net/19/8523/2019/, 2019.

Atkinson, R. and Arey, J.: Atmospheric degradation of volatile organic compounds, Chem. Rev., 103, 4605–4638, https://doi.org/10.1021/cr0206420, 2003.

Atkinson, R., Aschmann, S. M., Arey, J., and Carter, W. P.: Formation of ring-retaining products from the OH radical-initiated reactions of benzene and toluene, Int. J. Chem. Kinetics, 21, 801–827, 1989.

Barletta, B., Meinardi, S., Sherwood Rowland, F., Chan, C.-Y., Wang, X., Zou, S., Yin Chan, L., and Blake, D. R.: Volatile organic compounds in 43 Chinese cities, Atmos. Environ., 39, 5979–5990, 2005.

Bejan, I., El Aal, Y. A., Barnes, I., Benter, T., Bohn, B., Wiesen, P., and Kleffmann, J.: The photolysis of ortho-nitrophenols: a new gas phase source of HONO, Phys. Chem. Chem. Phys., 8, 2028–2035, 2006.

Birdsall, A. W., Andreoni, J. F., and Elrod, M. J.: Investigation of the role of bicyclic peroxy radicals in the oxidation mechanism of toluene, J. Phys. Chem. A, 114, 10 655–10 663, https://doi.org/10.1021/jp105467e, 2010.

Bloss, C., Wagner, V., Bonzanini, A., Jenkin, M. E., Wirtz, K., Martin-Reviejo, M., and Pilling, M. J.: Evaluation of detailed aromatic mechanisms (MCMv3 and MCMv3.1) against environmental chamber data, Atmos. Chem. Phys., 5, 623–639, https://doi.org/10.5194/acp-5-623-2005, https://www.atmos-chem-phys.net/5/623/2005/, 2005a.

Bloss, C., Wagner, V., Jenkin, M. E., Volkamer, R., Bloss, W. J., Lee, J. D., Heard, D. E., Wirtz, K., Martin-Reviejo, M., Rea, G., Wenger, J. C., and Pilling, M. J.: Development of a detailed chemical mechanism (MCMv3.1) for the atmospheric oxidation of aromatic hydrocarbons, Atmos. Chem. Phys., 5, 641–664, https://doi.org/10.5194/acp-5-641-2005, 2005b.

Cabrera-Perez, D., Taraborrelli, D., Sander, R., and Pozzer, A.: Global atmospheric budget of simple monocyclic aromatic compounds, Atmos. Chem. Phys., 16, 6931–6947, https://doi.org/10.5194/acp-16-6931-2016, 2016.

Carter, W. P. and Heo, G.: Development of revised SAPRC aromatics mechanisms, Atmospheric Environment, 77, 404 – 414, https://doi.org/https://doi.org/10.1016/j.atmosenv.2013.05.021, http://www.sciencedirect.com/science/article/pii/S1352231013003646, 2013.

Chen, J., Wenger, J. C., and Venables, D. S.: Near-ultraviolet absorption cross sections of nitrophenols and their potential influence on tropospheric oxidation capacity, J. Phys. Chem. A, 115, 12 235–12 242, https://doi.org/10.1021/jp206929r, 2011.

Cheng, S.-B., Zhou, C.-H., Yin, H.-M., Sun, J.-L., and Han, K.-L.: OH produced from o-nitrophenol photolysis: a combined experimental and theoretical investigation, J. Chem. Phys., 130, 234 311–234 311, https://doi.org/10.1063/1.3152635, 2009.

Daniel, J. S. and Solomon, S.: On the climate forcing of carbon monoxide, J. Geophys. Res., 103, 13 249–13 260, 1998.

Deckert, R., Jöckel, P., Grewe, V., Gottschaldt, K.-D., and Hoor, P.: A quasi chemistry-transport model mode for EMAC, Geosci. Model Dev., 4, 195–206, 2011.

Emmons, L. K., Walters, S., Hess, P. G., Lamarque, J.-F., Pfister, G. G., Fillmore, D., Granier, C., Guenther, A., Kinnison, D., Laepple, T., Orlando, J., Tie, X., Tyndall, G., Wiedinmyer, C., Baughcum, S. L., and Kloster, S.: Description and evaluation of the Model for Ozone and Related chemical Tracers, version 4 (MOZART-4), Geosci. Model Dev., 3, 43–67, https://doi.org/10.5194/gmd-3-43-2010, 2010.

Epstein, S. A., Riipinen, I., and Donahue, N. M.: A semiempirical correlation between enthalpy of vaporization and saturation concentration for organic aerosol, Environ. Sci. Technol., 44, 743–748, https://doi.org/10.1021/es902497z, 2010.

Field, R. J., Raghavan, N. V., and Brummer, J. G.: A pulse radiolysis investigation of the reactions of bromine dioxide radical (BrO2.cntdot.) with hexacyanoferrate(II), manganese(II), phenoxide ion, and phenol, The Journal of Physical Chemistry, 86, 2443–2449, https://doi.org/10.1021/j100210a040, https://doi.org/10.1021/j100210a040, 1982.

Fu, T.-M., Jacob, D. J., Wittrock, F., Burrows, J. P., Vrekoussis, M., and Henze, D. K.: Global budgets of atmospheric glyoxal and methylglyoxal, and implications for formation of secondary organic aerosols, J. Geophys. Res., 113D, 2008.

Guenther, A. B., Jiang, X., Heald, C. L., Sakulyanontvittaya, T., Duhl, T., Emmons, L. K., and Wang, X.: The Model of Emissions of Gases and Aerosols from Nature version 2.1 (MEGAN2.1): an extended and updated framework for modeling biogenic emissions, Geosci. Model Dev., 5, 1471–1492, https://doi.org/10.5194/gmd-5-1471-2012, 2012.

Heiden, A. C., Kobel, K., Komenda, M., Koppmann, R., Shao, M., and Wildt, J.: Toluene emissions from plants, Geophysical Research Letters, 26, 1283–1286, https://doi.org/https://doi.org/10.1029/1999GL900220, https://agupubs.onlinelibrary.wiley.com/doi/abs/10.1029/1999GL900220, 1999.

Henze, D., Seinfeld, J., Ng, N., Kroll, J., Fu, T.-M., Jacob, D. J., and Heald, C.: Global modeling of secondary organic aerosol formation from aromatic hydrocarbons: high-vs. low-yield pathways, Atmos. Chem. Phys., 8, 2405–2420, 2008.

Hoigné, J. and Bader, H.: Rate constants of reactions of ozone with organic and inorganic compounds in water—II: Dissociating organic compounds, Water Research, 17, 185 – 194, https://doi.org/https://doi.org/10.1016/0043-1354(83)90099-4, http://www.sciencedirect.com/science/article/pii/0043135483900994, 1983.

Holtslag, A. and Boville, B.: Local versus nonlocal boundary-layer diffusion in a global climate model, J. Clim., 6, 1825–1842, 1993.

Holtslag, A., De Bruijn, E., and Pan, H.: A high resolution air mass transformation model for short-range weather forecasting, Monthly Weather Review, 118, 1561–1575, 1990.

Hu, L., Millet, D. B., Baasandorj, M., Griffis, T. J., Travis, K. R., Tessum, C. W., Marshall, J. D., Reinhart, W. F., Mikoviny, T., Müller, M., Wisthaler, A., Graus, M., Warneke, C., and de Gouw, J.: Emissions of C_6–C_8 aromatic compounds in the United States: Constraints from tall tower and aircraft measurements, J. Geophys. Res., 120, https://doi.org/10.1002/2014JD022627, 2015.

Huang, G., Brook, R., Crippa, M., Janssens-Maenhout, G., Schieberle, C., Dore, C., Guizzardi, D., Muntean, M., Schaaf, E., and Friedrich, R.: Speciation of anthropogenic emissions of non-methane volatile organic compounds: a global gridded data set for 1970–2012, Atmos. Chem. Phys., 17, 7683–7701, https://doi.org/10.5194/acp-17-7683-2017, 2017.

Jagiella, S. and Zabel, F.: Reaction of phenylperoxy radicals with NO_2 at 298 K, Phys. Chem. Chem. Phys., 9, 5036–5051, https://doi.org/10.1039/B705193J, 2007.

Jenkin, M. E., Saunders, S. M., Wagner, V., and Pilling, M. J.: Protocol for the development of the Master Chemical Mechanism, MCM v3 (part B): tropospheric degradation of aromatic volatile organic compounds, Atmos. Chem. Phys., 3, 181–193, https://doi.org/10.5194/acp-3-181-2003, 2003.

Jöckel, P., Kerkweg, A., Pozzer, A., Sander, R., Tost, H., Riede, H., Baumgaertner, A., Gromov, S., and Kern, B.: Development cycle 2 of the Modular Earth Submodel System (MESSy2), Geosci. Model Dev., 3, 717–752, https://doi.org/10.5194/GMD-3-717-2010, 2010.

Jöckel, P., Tost, H., Pozzer, A., Kunze, M., Kirner, O., Brenninkmeijer, C. A. M., Brinkop, S., Cai, D. S., Dyroff, C., Eckstein, J., Frank, F., Garny, H., Gottschaldt, K.-D., Graf, P., Grewe, V., Kerkweg, A., Kern, B., Matthes, S., Mertens, M., Meul, S., Neumaier, M., Nützel, M., Oberländer-Hayn, S., Ruhnke, R., Runde, T., Sander, R., Scharffe, D., and Zahn, A.: Earth System Chemistry integrated Modelling (ESCiMo) with the Modular Earth Submodel System (MESSy), version 2.51, Geosci. Model Dev., 9, 1153–1200, https://doi.org/10.5194/gmd-9-1153-2016, 2016.

Kaiser, J. W., Heil, A., Andreae, M. O., Benedetti, A., Chubarova, N., Jones, L., Morcrette, J.-J., Razinger, M., Schultz, M. G., Suttie, M., and van der Werf, G. R.: Biomass burning emissions estimated with a global fire assimilation system based on observed fire radiative power, Biogeosci., 9, 527–554, https://doi.org/10.5194/bg-9-527-2012, 2012.

Koppmann, R.: Volatile organic compounds in the atmosphere, Blackwell Publishing Ltd, https://doi.org/10.1002/9780470988657, 2007.

Lamarque, J.-F., Bond, T. C., Eyring, V., Granier, C., Heil, A., Klimont, Z., Lee, D., Liousse, C., Mieville, A., Owen, B., Schultz, M. G., Shindell, D., Smith, S. J., Stehfest, E., Van Aardenne, J., Cooper, O. R., Kainuma, M., Mahowald, N., McConnell, J. R., Naik, V., Riahi, K., and van Vuuren, D. P.: Historical (1850–2000) gridded anthropogenic and biomass burning emissions of reactive gases and aerosols: methodology and application, Atmospheric Chemistry and Physics, 10, 7017–7039, https://doi.org/10.5194/acp-10-7017-2010, https://acp.copernicus.org/articles/10/7017/2010/, 2010.

Lee, S., Chiu, M., Ho, K., Zou, S., and Wang, X.: Volatile organic compounds (VOCs) in urban atmosphere of Hong Kong, Chemosphere, 48, 375–382, 2002.

Lelieveld, J. and Crutzen, P. J.: Influences of cloud photochemical processes on tropospheric ozone, Nature, 343, 227–233, https://doi.org/10.1038/343227A0, 1990.

Lelieveld, J., Gromov, S., Pozzer, A., and Taraborrelli, D.: Global tropospheric hydroxyl distribution, budget and reactivity, Atmos. Chem. Phys., 16, 12 477–12 493, https://doi.org/10.5194/acp-16-12477-2016, 2016.

Li, Y., Pöschl, U., and Shiraiwa, M.: Molecular corridors and parameterizations of volatility in the chemical evolution of organic aerosols, Atmos. Chem. Phys., 16, 3327–3344, https://doi.org/10.5194/acp-16-3327-2016, 2016.

Lin, G., Penner, J. E., Sillman, S., Taraborrelli, D., and Lelieveld, J.: Global modeling of SOA formation from dicarbonyls, epoxides, organic nitrates and peroxides, Atmos. Chem. Phys., 12, 4743–4774, https://doi.org/10.5194/acp-12-4743-2012, 2012.

Misztal, P., Hewitt, C., Wildt, J., Blande, J., Eller, A., Fares, S., Gentner, D., Gilman, J., Graus, M., Greenberg, J., Guenther, A., Hansel, A., Harley, P., Huang, M., Jardine, K., Karl, T., Kaser, L., Keutsch, F., Kiendler-Scharr, A., Kleist, E., Lerner, B., Li, T., Mak, J., Nölscher, A., Schnitzhofer, R., Sinha, V., Thornton, B., Warneke, C., Wegener, F., Werner, C., Williams, J., Worton, D., Yassaa, N., and Goldstein, A.: Atmospheric benzenoid emissions from plants rival those from fossil fuels, Scientific Reports, 5, https://doi.org/10.1038/srep12064, 2015.

Naik, V., Voulgarakis, A., Fiore, A. M., Horowitz, L. W., Lamarque, J.-F., Lin, M., Prather, M. J., Young, P. J., Bergmann, D., Cameron-Smith, P. J., Cionni, I., Collins, W. J., Dalsøren, S. B., Doherty, R., Eyring, V., Faluvegi, G., Folberth, G. A., Josse, B., Lee, Y. H., MacKenzie, I. A., Nagashima, T., van Noije, T. P. C., Plummer, D. A., Righi, M., Rumbold, S. T., Skeie, R., Shindell, D. T., Stevenson, D. S., Strode, S., Sudo, K., Szopa, S., and Zeng, G.: Preindustrial to present-day changes in tropospheric hydroxyl radical and methane lifetime from the Atmospheric Chemistry and Climate Model Intercomparison Project (ACCMIP), Atmospheric Chemistry and Physics, 13, 5277–5298, https://doi.org/10.5194/acp-13-5277-2013, https://acp.copernicus.org/articles/13/5277/2013/, 2013.

Ng, N. L., Kroll, J. H., Chan, A. W. H., Chhabra, P. S., Flagan, R. C., and Seinfeld, J. H.: Secondary organic aerosol formation from m-xylene, toluene, and benzene, Atmos. Chem. Phys., 7, 3909–3922, https://doi.org/10.5194/acp-7-3909-2007, 2007.

Patra, P. K., Krol, M. C., Montzka, S. A., Arnold, T., Atlas, E. L., Lintner, B. R., Stephens, B. B., Xiang, B., Elkins, J. W., Fraser, P. J., Ghosh, A., Hintsa, E. J., Hurst, D. F., Ishijima, K., Krummel, P. B., Miller, B. R., Miyazaki, K., Moore, F. L., Mühle, J., O'Doherty, S., Prinn, R. G., Steele, L. P., Takigawa, M., Wang, H. J., Weiss, R. F., Wofsy, S. C., and Young, D.: Observational evidence for interhemispheric hydroxyl-radical parity, Nature, 513, 219–223, https://doi.org/10.1038/nature13721, https://doi.org/10.1038/nature13721, 2014.

Paulot, F., Crounse, J. D., Kjaergaard, H. G., Kürten, A., St. Clair, J. M., Seinfeld, J. H., and Wennberg, P. O.: Unexpected epoxide formation in the gas-phase photooxidation of isoprene, Science, 325, 730–733, https://doi.org/10.1126/science.1172910, 2009.

Pozzer, A., Jöckel, P., Tost, H., Sander, R., Ganzeveld, L., Kerkweg, A., and Lelieveld, J.: Simulating organic species with the global atmospheric chemistry general circulation model ECHAM5/MESSy1: a comparison of model results with observations, Atmos. Chem. Phys., 7, 2527–2550, https://doi.org/10.5194/ACP-7-2527-2007, 2007.

Pozzer, A., Jöckel, P., and van Aardenne, J.: The influence of the vertical distribution of emissions on tropospheric chemistry, Atmos. Chem. Phys., 9, 9417–9432, https://doi.org/10.5194/ACP-9-9417-2009, 2009.

Pozzer, A., Pollmann, J., Taraborrelli, D., Jöckel, P., Helmig, D., Tans, P., Hueber, J., and Lelieveld, J.: Observed and simulated global distribution and budget of atmospheric C_2-C_5 alkanes, Atmos. Chem. Phys., 10, 4403–4422, https://doi.org/10.5194/ACP-10-4403-2010, 2010.

Pringle, K. J., Tost, H., Message, S., Steil, B., Giannadaki, D., Nenes, A., Fountoukis, C., Stier, P., Vignati, E., and Lelieveld, J.: Description and evaluation of GMXe: a new aerosol submodel for global simulations (v1), Geosci. Model Dev., 3, 391–412, https://doi.org/10.5194/gmd-3-391-2010, 2010.

Ran, L., Zhao, C., Geng, F., Tie, X., Tang, X., Peng, L., Zhou, G., Yu, Q., Xu, J., and Guenther, A.: Ozone photochemical production in urban Shanghai, China: Analysis based on ground level observations, J. Geophys. Res., 114D, 2009.

Roeckner, E., Brokopf, R., Esch, M., Giorgetta, M., Hagemann, S., Kornblueh, L., Manzini, E., Schlese, U., and Schulzweida, U.: Sensitivity of simulated climate to horizontal and vertical resolution in the ECHAM5 atmosphere model, J. Clim., 19, 3771–3791, https://doi.org/10.1175/JCLI3824.1, 2006.

Rosanka, S., Sander, R., Wahner, A., and Taraborrelli, D.: Oxidation of low-molecular weight organic compounds in cloud droplets: development of the JAMOC chemical mechanism in CAABA/MECCA (version 4.5.0gmdd), Geoscientific Model Development Discussions, 2020, 1–18, https://doi.org/10.5194/gmd-2020-337, https://gmd.copernicus.org/preprints/gmd-2020-337/, 2020.

Roth, E., Chakir, A., and Ferhati, A.: Study of a benzoylperoxy radical in the gas phase: ultraviolet spectrum and $C_6H_5C(O)O_2$ + HO_2 reaction between 295 and 357 K, J. Phys. Chem. A, 114, 10 367–10 379, https://doi.org/10.1021/jp1021467, 2010.

Sack, T. M., Steele, D. H., Hammerstrom, K., and Remmers, J.: A survey of household products for volatile organic compounds, Atmos. Environ., 26A, 1063–1070, 1992.

Sander, R., Jöckel, P., Kirner, O., Kunert, A. T., Landgraf, J., and Pozzer, A.: The photolysis module JVAL-14, compatible with the MESSy standard, and the JVal PreProcessor (JVPP), Geosci. Model Dev., 7, 2653–2662, https://doi.org/10.5194/GMD-7-2653-2014, 2014.

Sander, R., Baumgaertner, A., Cabrera-Perez, D., Frank, F., Gromov, S., Grooß, J.-U., Harder, H., Huijnen, V., Jöckel, P., Karydis, V. A., Niemeyer, K. E., Pozzer, A., Riede, H., Schultz, M. G., Taraborrelli, D., and Tauer, S.: The community atmospheric chemistry box model CAABA/MECCA-4.0, Geosci. Model Dev., 12, 1365–1385, https://doi.org/10.5194/gmd-12-1365-2019, 2019.

Sherwen, T., Schmidt, J. A., Evans, M. J., Carpenter, L. J., Großmann, K., Eastham, S. D., Jacob, D. J., Dix, B., Koenig, T. K., Sinreich, R., Ortega, I., Volkamer, R., Saiz-Lopez, A., Prados-Roman, C., Mahajan, A. S., and Ordóñez, C.: Global impacts of tropospheric halogens (Cl, Br, I) on oxidants and composition in GEOS-Chem, Atmospheric Chemistry and Physics, 16, 12 239–12 271, https://doi.org/10.5194/acp-16-12239-2016, https://www.atmos-chem-phys.net/16/12239/2016/, 2016.

Sillman, S., Logan, J. A., and Wofsy, S. C.: The sensitivity of ozone to nitrogen oxides and hydrocarbons in regional ozone episodes, J. Geophys. Res., 95D, 1837–1851, https://doi.org/10.1029/JD095iD02p01837, 1990.

Tao, Z. and Li, Z.: A kinetics study on reactions of C_6H_5O with C_6H_5O and O_3 at 298 K, Int. J. Chem. Kinet., 31, 65–72, https://doi.org/10.1002/(SICI)1097-4601(1999)31:1<65::AID-KIN8>3.0.CO;2-J, 1999.

Taraborrelli, D., Lawrence, M. G., Butler, T. M., Sander, R., and Lelieveld, J.: Mainz Isoprene Mechanism 2 (MIM2): an isoprene oxidation mechanism for regional and global atmospheric modelling, Atmos. Chem. Phys., 9, 2751–2777, https://doi.org/10.5194/ACP-9-2751-2009, 2009.

Tarr, M. A., Miller, W. L., and Zepp, R. G.: Direct carbon monoxide photoproduction from plant matter, Journal of Geophysical Research: Atmospheres, 100, 11 403–11 413, https://doi.org/https://doi.org/10.1029/94JD03324, https://agupubs.onlinelibrary.wiley.com/doi/abs/10.1029/94JD03324, 1995.

Tilmes, S., Lamarque, J.-F., Emmons, L. K., Kinnison, D. E., Marsh, D., Garcia, R. R., Smith, A. K., Neely, R. R., Conley, A., Vitt, F., Val Martin, M., Tanimoto, H., Simpson, I., Blake, D. R., and Blake, N.: Representation of the Community Earth System Model (CESM1) CAM4-chem within the Chemistry-Climate Model Initiative (CCMI), Geoscientific Model Development, 9, 1853–1890, https://doi.org/10.5194/gmd-9-1853-2016, https://www.geosci-model-dev.net/9/1853/2016/, 2016.

Tost, H., Jöckel, P., Kerkweg, A., Sander, R., and Lelieveld, J.: Technical note: A new comprehensive SCAVenging submodel for global atmospheric chemistry modelling, Atmos. Chem. Phys., 6, 565–574, https://doi.org/10.5194/ACP-6-565-2006, 2006.

Tost, H., Lawrence, M. G., Brühl, C., Jöckel, P., The GABRIEL Team, and The SCOUT-O3-DARWIN/ACTIVE Team: Uncertainties in atmospheric chemistry modelling due to convection parameterisations and subsequent scavenging, Atmos. Chem. Phys., 10, 1931–1951, https://doi.org/10.5194/ACP-10-1931-2010, 2010.

Troen, I. and Mahrt, L.: A simple model of the atmospheric boundary layer; sensitivity to surface evaporation, Boundary-Layer Meteorology, 37, 129–148, 1986.

Tsimpidi, A. P., Karydis, V. A., Pozzer, A., Pandis, S. N., and Lelieveld, J.: ORACLE (v1.0): module to simulate the organic aerosol composition and evolution in the atmosphere, Geosci. Model Dev., 7, 3153–3172, https://doi.org/10.5194/gmd-7-3153-2014, 2014.

Tyndall, G. S., Wallington, T. J., and Ball, J. C.: FTIR Product Study of the Reactions CH3O2 + CH3O2 and CH3O2 + O3, The Journal of Physical Chemistry A, 102, 2547–2554, https://doi.org/10.1021/jp972784h, https://doi.org/10.1021/jp972784h, 1998.

van der Werf, G. R., Randerson, J. T., Giglio, L., van Leeuwen, T. T., Chen, Y., Rogers, B. M., Mu, M., van Marle, M. J. E., Morton, D. C., Collatz, G. J., Yokelson, R. J., and Kasibhatla, P. S.: Global fire emissions estimates during 1997–2016, Earth System Science Data, 9, 697–720, https://doi.org/10.5194/essd-9-697-2017, https://www.earth-syst-sci-data.net/9/697/2017/, 2017.

Vereecken, L.: Reaction Mechanisms for the Atmospheric Oxidation of Monocyclic Aromatic Compounds, chap. Chapter 6, pp. 377–527, World Scientific Publishing, https://doi.org/10.1142/9789813271838_0006, https://www.worldscientific.com/doi/abs/10.1142/9789813271838_0006, 2019.

Vereecken, L., Chakravarty, H. K., Bohn, B., and Lelieveld, J.: Theoretical Study on the Formation of H- and O-Atoms, HONO, OH, NO, and NO2 from the Lowest Lying Singlet and Triplet States in Ortho-Nitrophenol Photolysis, International Journal of Chemical Kinetics, 48, 785–795, https://doi.org/10.1002/kin.21033, https://onlinelibrary.wiley.com/doi/abs/10.1002/kin.21033, 2016.

Volkamer, R., Platt, U., and Wirtz, K.: Primary and secondary glyoxal formation from aromatics: Experimental evidence for the bicycloalkyl-radical pathway from benzene, toluene, and p-xylene, J. Phys. Chem. A, 105, 7865–7874, https://doi.org/10.1021/jp010152w, 2001.

Wallington, T. J., Ammann, M., Cox, R. A., Crowley, J. N., Herrmann, H., Jenkin, M. E., McNeill, V., Mellouki, A., Rossi, M. J., and Troe, J.: IUPAC Task group on atmospheric chemical kinetic data evaluation: Evaluated kinetic data, http://iupac.pole-ether.fr, 2018.

Warneck, P.: Chemistry of the Natural Atmosphere, second edition, Academic Press, 1999.

WMO: Definition of the tropopause and of significant levels, https://library.wmo.int/doc_num.php?explnum_id=6960, 1957.

WMO: Air quality guidelines for Europe, Copenhagen: WHO Regional Office for Europe, 2000.

Yan, Y., Lin, J., Chen, J., and Hu, L.: Improved simulation of tropospheric ozone by a global-multi-regional two-way coupling model system, Atmospheric Chemistry and Physics, 16, 2381–2400, https://doi.org/10.5194/acp-16-2381-2016, https://acp.copernicus.org/articles/16/2381/2016/, 2016.

Yan, Y., Cabrera-Perez, D., Lin, J., Pozzer, A., Hu, L., Millet, D. B., Porter, W. C., and Lelieveld, J.: Global tropospheric effects of aromatic chemistry with the SAPRC-11 mechanism implemented in GEOS-Chem version 9-02, Geosci. Model Dev., 12, 111–130, https://doi.org/10.5194/gmd-12-111-2019, 2019.

Young, P. J., Naik, V., Fiore, A. M., Gaudel, A., Guo, J., Lin, M., Neu, J., Parrish, D., Reider, H., Schnell, J., et al.: Tropospheric Ozone Assessment Report: Assessment of global-scale model performance for global and regional ozone distributions, variability, and trends, Elementa: Science of the Anthropocene, 6, 2018.